



HAL
open science

Influence of TiO₂ nanocomposite UV filter surface chemistry and their interactions with organic UV filters on uptake and toxicity toward cultured fish gill cells

Nicolas Martin, Britt Wassmur, Danielle Slomberg, Jérôme Labille, Tobias Lammel

► To cite this version:

Nicolas Martin, Britt Wassmur, Danielle Slomberg, Jérôme Labille, Tobias Lammel. Influence of TiO₂ nanocomposite UV filter surface chemistry and their interactions with organic UV filters on uptake and toxicity toward cultured fish gill cells. *Ecotoxicology and Environmental Safety*, 2022, 243, pp.113984. 10.1016/j.ecoenv.2022.113984 . hal-03876913

HAL Id: hal-03876913

<https://hal.science/hal-03876913>

Submitted on 29 Nov 2022

HAL is a multi-disciplinary open access archive for the deposit and dissemination of scientific research documents, whether they are published or not. The documents may come from teaching and research institutions in France or abroad, or from public or private research centers.

L'archive ouverte pluridisciplinaire **HAL**, est destinée au dépôt et à la diffusion de documents scientifiques de niveau recherche, publiés ou non, émanant des établissements d'enseignement et de recherche français ou étrangers, des laboratoires publics ou privés.



Distributed under a Creative Commons Attribution 4.0 International License



Influence of TiO₂ nanocomposite UV filter surface chemistry and their interactions with organic UV filters on uptake and toxicity toward cultured fish gill cells

Nicolas Martin^a, Britt Wassmur^a, Danielle Slomberg^b, Jérôme Labille^b, Tobias Lammel^{a,*}

^a Department of Biological and Environmental Sciences, University of Gothenburg, Sweden

^b Aix-Marseille University, CNRS, IRD, INRAe, Coll. France, CEREGE, Aix-en-Provence, France

ARTICLE INFO

Keywords:
Nanoparticle
Mixture
in vitro
Ecotoxicity
Sunscreen
Interference

ABSTRACT

Aquatic environments have been found to be contaminated with a variety of inorganic and organic UV filters. This includes novel nano-sized titanium dioxide (TiO₂) composite particles, which have been increasingly developed and incorporated into commercial sunscreens in recent years. So far, relatively little is known about the effects of this novel class of UV filters on aquatic life. Therefore, this study aimed to determine and compare the toxicity of three such nanoparticulate TiO₂ UV filters with different surface coatings, namely Eusolex® T-Avo (SiO₂-coated), T-Lite™ SF (Al(OH)₃/PDMS-coated), and Eusolex® T-S (Al₂O₃/stearic acid-coated) either alone, or in the presence of selected organic UV filters (octinoxate, avobenzone, octocrylene), toward fish using RTgill-W1 cell cultures as an in vitro experimental model. Besides standard exposure protocols, alternative approaches (i.e., exposure to water accommodated fractions (WAFs), hanging-drop exposure) were explored to account for nanoparticle (NP)-specific fate in the medium and obtain additional/complementary information on their toxicity in different conditions. The AlamarBlue, CFDA-AM and Neutral Red Retention (NR) assays were used to measure effects on different cellular endpoints. Transmission electron microscopy (TEM) was used to examine NP uptake. Our results showed that none of the TiO₂ NP UV filters were cytotoxic at the concentrations tested (0.1–10 µg/mL; 24 h) but there were differences in their uptake by the cells. Thus, only the hydrophilic T-AVO was detected inside cells, but the hydrophobic T-Lite SF and T-S were not. In addition, our results show that the presence of NPs (or the used dispersant) tended to decrease organic UV filter toxicity. The level of combination effect depended on both NP-type (surface chemistry) and concentration, suggesting that the reduced toxicity resulted from reduced availability of the organic UV filters due to their adsorption to the NP surface. Thus, mixtures of TiO₂ NP UV filters and organic UV filters may have a different toxicological profile compared to the single substances, but probably do not pose an increased hazard.

1. Introduction

Humans use sunscreens to protect their skin from excessive exposure to solar ultraviolet (UV) radiation, which can lead to harmful effects, such as burning, premature skin aging or skin cancer. The first commercial sunscreen was developed in the 1920s (Urbach, 2001), and, with the increase in coastal tourism, sunscreen production has augmented ever since (Tovar-Sánchez et al., 2013). UV filter substances used in sunscreen formulations today are organic or inorganic in nature, and, attenuate UV radiation by different processes including absorption, scattering or reflection (Egambaram et al., 2020). Often, they are incorporated into sunscreens in the form of a complex mixture to ensure

i) efficient protection against a broad spectrum of UV radiation (Chatelain and Gabard, 2001; Gaspar and Maia Campos, 2006), and ii) photostability of the active ingredients/product (Villalobos-Hernández and Müller-Goymann, 2006; Wissing and Müller, 2001).

The continuous and wide use of organic and inorganic UV filters in sunscreens and other personal care products inevitably leads to their entry into the aquatic environment. Sunscreens can be washed off the skin during recreational activities/swimming into natural water bodies (direct release), or during showering/washing and subsequent discharge from sewage treatment plants (STPs) (indirect release) (Johnson et al., 2011; Jurado et al., 2014; Ramos et al., 2016; Sánchez-Quiles and Tovar-Sánchez, 2015; Tsui et al., 2014). Organic and inorganic UV filters

* Corresponding author.

E-mail address: tobias.lammel@gu.se (T. Lammel).

<https://doi.org/10.1016/j.ecoenv.2022.113984>

Received 21 December 2021; Received in revised form 28 June 2022; Accepted 14 August 2022

Available online 19 August 2022

0147-6513/© 2022 The Authors. Published by Elsevier Inc. This is an open access article under the CC BY license (<http://creativecommons.org/licenses/by/4.0/>).

have been detected in both freshwater and seawater environments with strong anthropogenic pressure but also in remote areas such as the Tuamotu Archipelago, Arctic and Antarctic sea, and concentration levels were found to vary considerably depending on not only the geographic region, but also the water layer, and season (Emnet et al., 2015; Goksøyr et al., 2009; Gondikas et al., 2018, 2014; Labille et al., 2020; Reed et al., 2017; Sánchez Rodríguez et al., 2015; Tsui et al., 2014). Their widespread presence and increasing release into the aquatic environment classifies them as emerging contaminants, and calls for a thorough assessment of their (eco)toxicity (Liu and Wong, 2013; Ramos et al., 2015).

Organic UV filters are comparatively well studied. Due their lipophilicity they have a high potential to bioaccumulate and biomagnify in aquatic food webs (Gago-Ferrero et al., 2012). Acute and chronic exposure to the parent compounds and their degradation products can have adverse effects on organisms (Kunz and Fent, 2006; Schlumpf et al., 2001). Some of the most commonly used organic UV filters, such as octinoxate (2-ethylhexyl trans-4-methoxycinnamate) and avobenzene (butyl bethoxydibenzoylmethane), have already been banned in certain geographic regions, mainly because of their demonstrated impacts on coral reefs (DiNardo and Downs, 2018; Gago-Ferrero et al., 2012), but effects in aquatic vertebrates, specifically fish, have also been observed, including impaired reproduction (Kim and Choi, 2014), and behavioural and morphological abnormalities (Araújo et al., 2018; Barone et al., 2019; Carvalhais et al., 2021). Octinoxate was also included in the European Chemicals Agency (ECHA) Community Rolling Action Plan (CoRAP) and is being re-evaluated because of its suspected PBT (persistent bioaccumulative, toxic) and endocrine disrupting properties (Ylä-Mononen, 2018).

Titanium dioxide (TiO₂) is one of the most common inorganic UV filter substances used in sunscreen formulations. It may be used in bulk form but is increasingly included in nano-particulate (≤ 100 nm) form (NPs) because of the relatively higher UV protective effect and aesthetic properties (Osterwalder et al., 2014). TiO₂ NP UV filters are often surface-coated with one or multiple layers of another inorganic or organic material (Faure et al., 2013), that is, they are composite materials and hence differ from TiO₂ NPs that may be naturally present in the environment. This coating serves to improve their stability, facilitate their incorporation in sunscreens, and mitigate undesired photocatalytic effects (phototoxicity) on cells and organisms observed for bare TiO₂ NPs, in particular anatase (Horie et al., 2016; Jovanovic, 2015; Sanders et al., 2012; Tang et al., 2018; Xiong et al., 2013; Yin et al., 2012). These differences in the surface coating/chemistry are likely to affect their behaviour and fate in the aquatic environment (e.g., agglomeration and sedimentation) (Slomberg et al., 2021), and also their interaction with surface epithelia of aquatic organisms, and thus their uptake, accumulation and toxicity (Catalano et al., 2020a; Liu et al., 2019; Turan et al., 2019).

So far, little research has been carried out assessing the toxicity of nano-composite TiO₂ NP UV filters in fish (for example, Fouqueray et al., 2013). However, there is a comparatively large body of literature on the effects of other types of TiO₂ NPs (e.g., TiO₂ P25) showing that they may be taken up following waterborne and dietary exposure, and may reach and be retained in vital organs including gill and liver, where they may interact and be internalised by cells, induce oxidative stress, and cause organ pathologies (Diniz et al., 2013; Federici et al., 2007; Hao et al., 2009; Johnston et al., 2010; Lammel et al., 2019a, 2019b; Lammel and Sturve, 2018; Reeves et al., 2008; Shi et al., 2016; Wang et al., 2016; Xiong et al., 2011). Furthermore, there is an increasing body of literature suggesting that TiO₂ NPs can adsorb toxic metals (e.g., Cd, Pb, As) and organic pollutants (e.g., PFAS, PCBs, pesticides) to their surface reducing their bioavailability or facilitating their uptake depending on the experimental conditions and model used in the study (Ilna et al., 2017; Li et al., 2020; Miao et al., 2015; Qiang et al., 2016; Sun et al., 2007; Zhang et al., 2007).

The overall aim of the present study was to assess the toxicity of

novel TiO₂ NP UV filters, and their interaction and combined effects with organic UV filter compounds, with which they are likely to be released together and co-exist in the aquatic environment. The specific objectives of this work were: (1) To determine the relative cytotoxic potential of three TiO₂ NP UV filters coated with different materials (i.e., nano-composites), namely, T-AVO (coated with silica), T-Lite (coated with aluminium hydroxide and PDMS), and T-S (coated with alumina and stearic acid) to fish gill cells, and compare it with that caused by the three commonly used organic UV filters avobenzene, octinoxate, and octocrylene; (2) To assess if exposure to binary mixtures of these two types of UV filters (i.e., TiO₂ NP UV filters and organic UV filters) can result in combination effects that differ from that caused by the mixture components alone.

Testing was performed using the permanent Rainbow trout gill cell line RTgill-W1 as experimental model adopting two different approaches. In the first approach the cell cultures were dosed to freshly prepared NP dispersions (alone and in mixtures with organic UV filters). In the second approach the cell cultures were exposed to only the water accommodated fraction (WAF) of the NP dispersions (and NP-chemical mixtures).

2. Materials and methods

2.1. Laboratory chemicals and reagents

The chemicals used to prepare L-15/ex, that is, sodium chloride (NaCl), potassium chloride (KCl), magnesium chloride (MgCl₂ x 6 H₂O), magnesium sulfate (MgSO₄ x 7 H₂O), calcium chloride (CaCl₂ x 2 H₂O), sodium phosphate monobasic (Na₂HPO₄), sodium pyruvate and galactose were from Sigma-Aldrich (Merck KGaA). The ultrapure water (resistivity of 18.2 M Ω ·cm at 25 °C) was obtained from the in-house Millipore Milli-Q Academic Ultra Pure Water Purification System. The biochemical reagents used in cell viability assays were purchased from ThermoFisher Scientific (AlamarBlue HS solution and 5-carboxyfluorescein diacetate, acetoxymethyl ester (CFDA-AM)) and Sigma-Aldrich (Neutral Red solution (0.33%)). Dimethylsulfoxide (DMSO), which was used as a solvent to prepare chemical stock solutions, was from Sigma-Aldrich.

2.2. Test substances

2.2.1. Organic UV filters

Avobenzene (IUPAC name: 3-(4-*tert*-Butylphenyl)-1-(4-methoxyphenyl)propane-1,3-dione; Trade name: Parsol®1789) and octinoxate (IUPAC name: 2-ethylhexyl 3-(4-methoxyphenyl)prop-2-enoate; Trade name: Parsol®MCX) were from Givaudan-Roure (Surrey, UK). Octocrylene (IUPAC name: 2-Propenoic acid, 2-cyano-3,3-diphenyl-, 2-ethylhexyl ester) was from Sigma-Aldrich. Stock solutions of the organic UV filters were prepared in DMSO with a concentration of 100 mM, aliquoted and stored in Eppendorf tubes at -18 °C until used in experiments.

2.2.2. Nanoparticulate TiO₂ UV filters

Three TiO₂ nano-composites (T-AVO®, T-Lite™ SF, and T-S®), manufactured as commercial UV filters for use in sunscreens, were selected based on their different surface chemistries. T-AVO is hydrophilic, and T-Lite SF and T-S are hydrophobic. To be more specific, T-AVO (Eusolex® line, Merck, Germany) consists of a TiO₂ core of nanometric rods (~30–80 × ~15–20 nm (Slomberg et al., 2021)) coated with a SiO₂ layer to protect against TiO₂ photocatalytic activity. T-Lite™ SF (BASF, Germany) is coated with an Al(OH)₃ passivation layer and a secondary polydimethylsiloxane (PDMS) layer to aid in dispersion in oil phases. According to the manufacturer, the nano-metric rods of the TiO₂ core measure 10 × 50 nm. T-S® (Eusolex® line, Merck, Germany), with a core of 60–100 × 15–20 nm, is coated with Al₂O₃ to prevent TiO₂ photocatalytic effects and a secondary layer of stearic acid to aid in

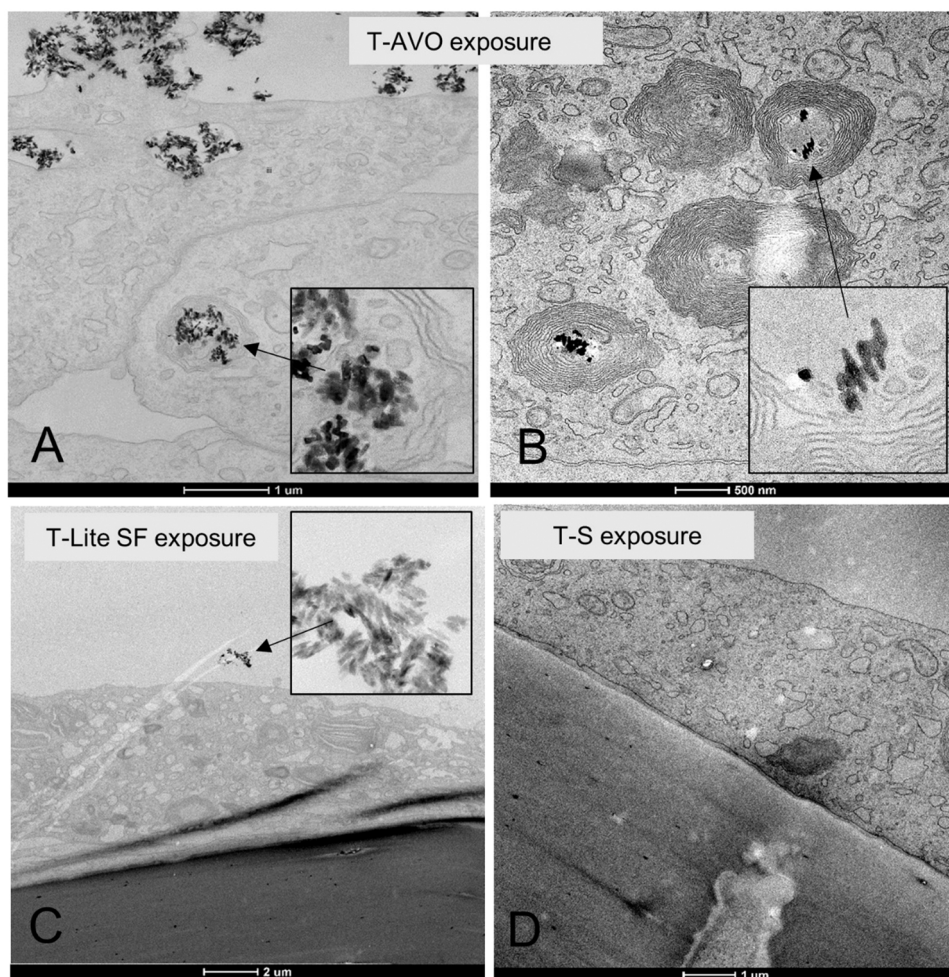


Fig. 1. TEM images of RTgill-W1 cells following exposure to TiO₂ NP UV filters (10 µg/mL, 24 h). Cellular uptake was observed for T-AVO (A and B) but not for T-Lite SF (C) and T-S (D). Inserts show NP agglomerates observed inside and outside cells as enlarged image (close-up). Scale bars in A, B, C and D are 1 µm, 500 nm, 2 µm and 1 µm, respectively.

dispersion.

TiO₂ NP UV filter stock dispersions were prepared as follows. T-AVO was dispersed in Milli-Q water at 10 mg/mL and T-Lite SF and T-S were dispersed in oil at 10 mg/mL. The oil phase used here is representative of that found in water-in-oil (w/o) emulsion sunscreens, and was prepared by mixing coco-caprylate (Cetiol-LC®; BASF SE, Germany), isopropyl palmitate (Tego-soft P®; Evonik Nutrition & Care GmbH, Germany), and an emulsifier (EASYNVOV™; SEPPIC, France) in a ratio of 2:2:1 for 24 h with magnetic stirring at 200 rpm, as previously described and used by Catalano et al. (2020b).

2.3. Characterisation of nanoparticulate TiO₂ UV filters

2.3.1. Transmission electron microscopy

TEM grids were drop-coated with T-AVO, T-Lite SF, and TS dispersions in L-15/ex (10 µg/mL) immediately after preparation, and thereafter imaged using a Talos L120C transmission electron microscope (FEL, Thermo Scientific) equipped with a 4 × 4k CMOS Ceta camera.

2.3.2. Dynamic light scattering analysis

The hydrodynamic diameter and colloidal stability of T-AVO, T-Lite SF and T-S during the cell exposure were analysed by dynamic light scattering (DLS) using a Zetasizer Nano-ZS apparatus (Malvern Instruments Ltd., Malvern, UK). The NP dispersions and controls (blanks) were prepared in the same way as for toxicity testing (described below). DLS analysis was performed immediately (~1 h) after preparation of the

dispersions, as well as after 24 h of incubation at 20 °C in static conditions, to obtain information on the NP properties at the beginning and end of the exposure. For all samples, four consecutive measurements at ten runs were conducted at 20 °C using 173° back scatter detection (after an initial temperature calibration of 120 s). The attenuation level and optimum measurement position was automatically set by the instrument. The results were calculated using the general purpose (normal resolution) analysis model (Zetasizer software version 7.11, Malvern Instruments Ltd.).

The same instrument (Zetasizer Nano-ZS apparatus) was used to measure the electrophoretic mobility of the three TiO₂ nano-composites in L-15/ex. Following 120 s of calibration time, three consecutive measurements at 20 °C were performed on each sample. All other measurement parameters, including the number of required runs per measurement, measurement position, attenuator level, and applied voltage was automatically determined and set by the instrument. The zeta-potential was computed using the Smoluchowski model (Zetasizer software version 7.11, Malvern Instruments Ltd.).

2.4. Cell line and routine cell culture

The cell line used in this study was the RTgill-W1 cell line, which is an epithelial cell line that was established from gill explants of adult rainbow trout (*Oncorhynchus mykiss*) (Bols et al., 1994). RTgill-W1 cells were cultured in 75 cm² cell culture flasks (TC Flask T75, Sarstedt) in phenol red-free Leibovitz's L-15 Medium supplemented with 5% fetal

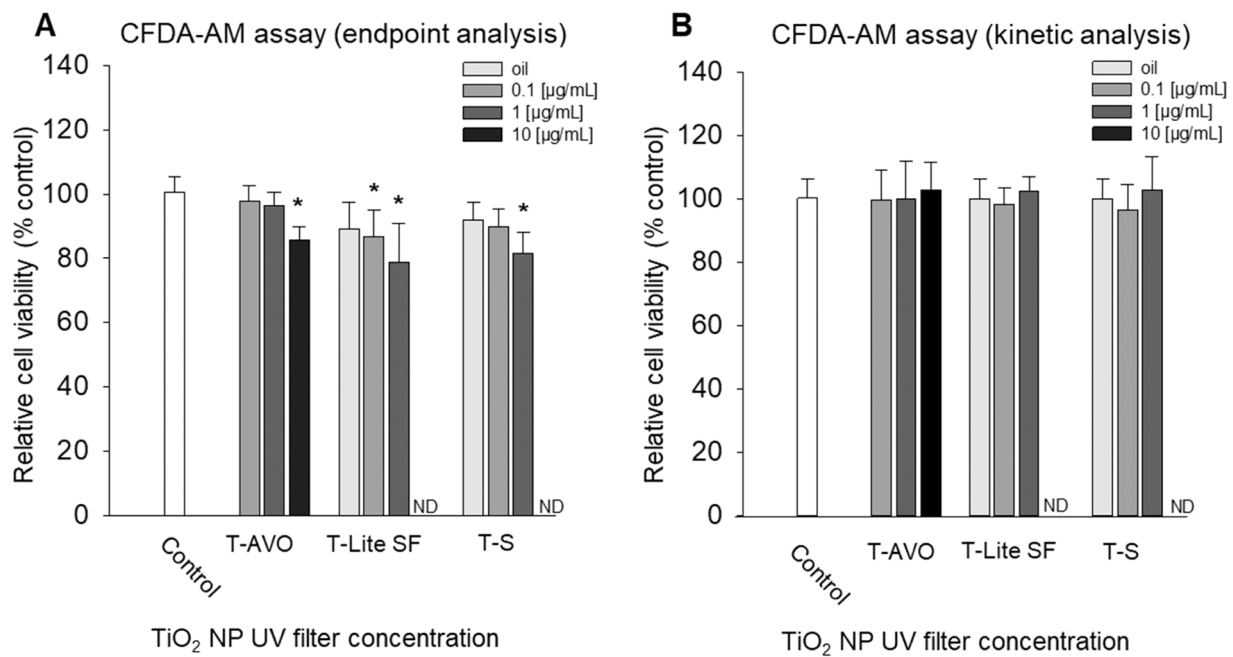


Fig. 2. Effect of the TiO₂ NP UV filters T-AVO, T-Lite SF and T-S on RTgill-W1 cell viability as determined by the CFDA-AM assay. A) Results obtained using the standard protocol (endpoint analysis). B) Results obtained using the modified protocol (kinetic analysis). Bars and error bars show means and SD of nine independent experimental replicates (n = 9). Asterisks (*) indicate statistically significant differences (p < 0.05) compared to the “control” (unexposed cells) (ANOVA on ranks followed by Tuckey method). Note that the highest exposure concentration of T-Lite SF and T-S was 1 µg/mL (the “missing” 10 µg/mL treatments are indicated as ND = not determined).

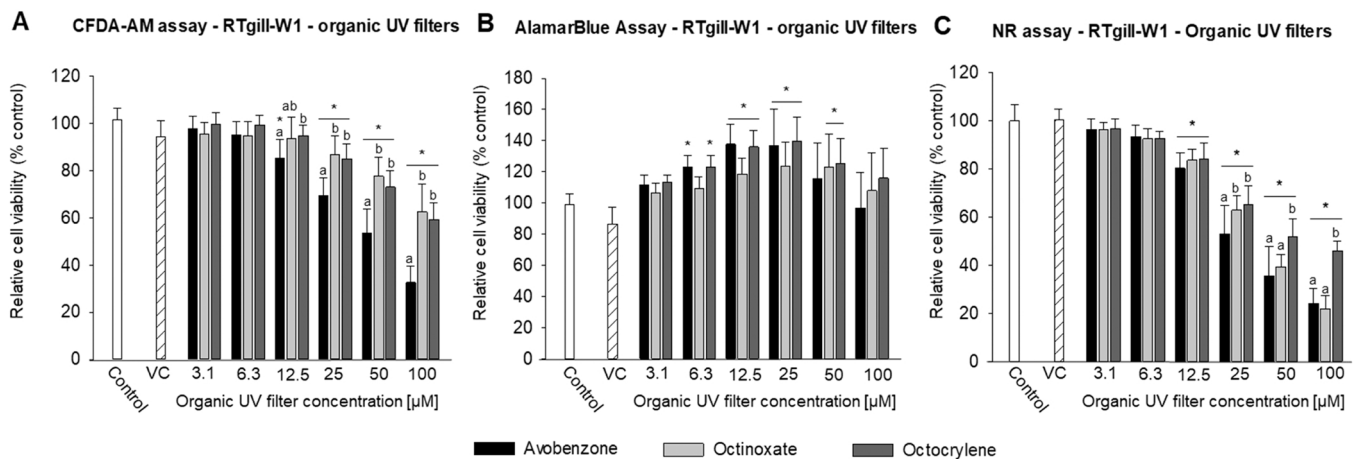


Fig. 3. Effect of the organic UV filters avobenzene, octinoxate, and octocrylene on RTgill-W1 cell viability. A) CFDA-AM assay results, B) AlamarBlue assay results, C) NR assay results. Bars and error bars show means and SD of nine independent experimental replicates (n = 9). VC is the vehicle control corresponding to 0.1% of DMSO. Statistically significant differences between treatment groups are indicated by different letters (One-way ANOVA followed by multiple comparison using Holm-Sidak method, p < 0.05 for CFDA-AM and NR assay data, and a One-way ANOVA on ranks for AlamarBlue assay data). Asterisks (*) indicate statistically significant differences (p < 0.05) compared to the control (One-way ANOVA followed by multiple comparison using Holm-Sidak method, p < 0.05 for CFDA-AM and NR assay data, and a one way ANOVA on ranks followed by Dunn’s method of comparison for AlamarBlue assay data). 100 µM of avobenzene, octinoxate, and octocrylene correspond to 31 µg/mL, 29 µg/mL, and 36 µg/mL, respectively.

bovine serum (FBS) (both from Gibco, Thermo Fisher Scientific). The flasks were incubated at 19 °C and split in ratios of 1:2 or 1:3 when reaching confluence using phosphate buffered saline (PBS) (prepared in-house) containing 0.2 g/l ethylenediaminetetraacetic acid (EDTA) (Sigma-Aldrich), and 0.25% trypsin-EDTA solution (Gibco).

2.5. Study of interaction of TiO₂ NP UV filters with RTgill-W1 cell monolayer cultures

2.5.1. Seeding and culture of RTgill-W1 cells in ThinCert® cell culture inserts

Epithelial cells cultured as a monolayer on permeable membrane supports placed into multi-well plates (so-called cell culture inserts) which divide the well into an upper and a lower compartment can be used as an in vitro model to study transport/translocation of chemical substances across fish epithelia. In this study, we tried to reproduce such

Table 1
Toxicological dose descriptors of TiO₂ NP UV filter and organic UV filter cytotoxicity in RTgill-W1 cells based on NR assay data.

UV filter name	LOEC [mg/L]	EC50 [mg/L]	Water solubility [mg/L]
Avobenzone	3.9	10.2 ± 0.6	*2.2 (25 °C)
Octinoxate	3.6	11.0 ± 0.4	*0.2–0.8 (21 °C)
Octocrylene	4.5	23.6 ± 1.9	*insoluble
T-AVO	** > 10	ND	NA
T-Lite SF	** > 10	ND	NA
T-S	** > 10	ND	NA

* retrieved from <https://pubchem.ncbi.nlm.nih.gov/>; ** Concentration tested in pilot experiments. NA = not applicable. ND = not determined. EC50 values are given as mean ± SD.

a model using RTgill-W1 cells and use it to study the interaction of TiO₂ NP UV filters with the fish gill epithelium in vitro. ThinCert® cell culture inserts for 12-well plates (Greiner Bio-One) were seeded with RTgill-W1 cells suspended in L-15 medium supplemented with 5% FBS and 1% penicillin-streptomycin (10,000 U/mL, Gibco) (200,000 cells/insert), and then incubated overnight at 19 °C to allow cell attachment and spreading. The next day, the medium in the upper compartment (i.e., the insert) was replaced by L-15/ex (a minimal version of the L-15 medium used for routine cell culture (see above) that only contains the salts NaCl, KCl, MgSO₄, MgCl₂, CaCl₂, Na₂HPO₄ and sodium pyruvate and galactose (Schirmer et al., 1997)), and the plates were placed back in the incubator where they were kept for three weeks, with the medium in the lower and upper compartment being replaced once per week. Formation of tight monolayer cell sheets was monitored measuring transepithelial electrical resistance (TEER) at regular time intervals (2, 4, 7, 11, 13, 17, and 21 days post seeding) using a chopstick electrode set connected to a

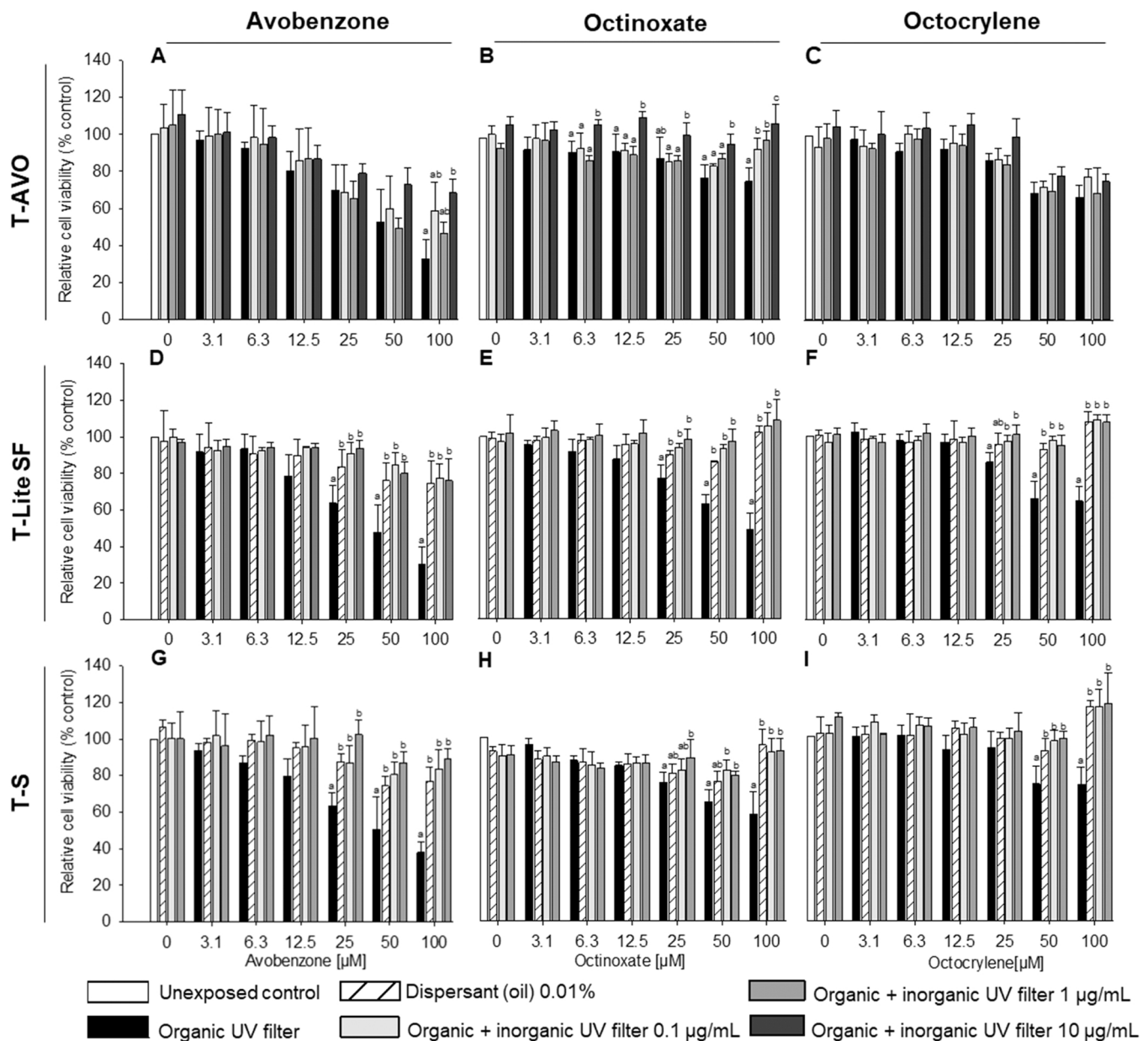


Fig. 4. Effects on RTgill-W1 cell viability following exposure to binary mixtures of TiO₂ NP UV filters and organic UV filters as determined by the CFDA-AM assay (kinetic analysis). Bars and error bars show the mean and SD of three independent experimental replicates (n = 3). Letters above bars denote statistically significant differences between treatments with and without TiO₂ NPs (different concentrations) (One-way ANOVA followed by Holm-Sidak multiple comparison test, p < 0.05).

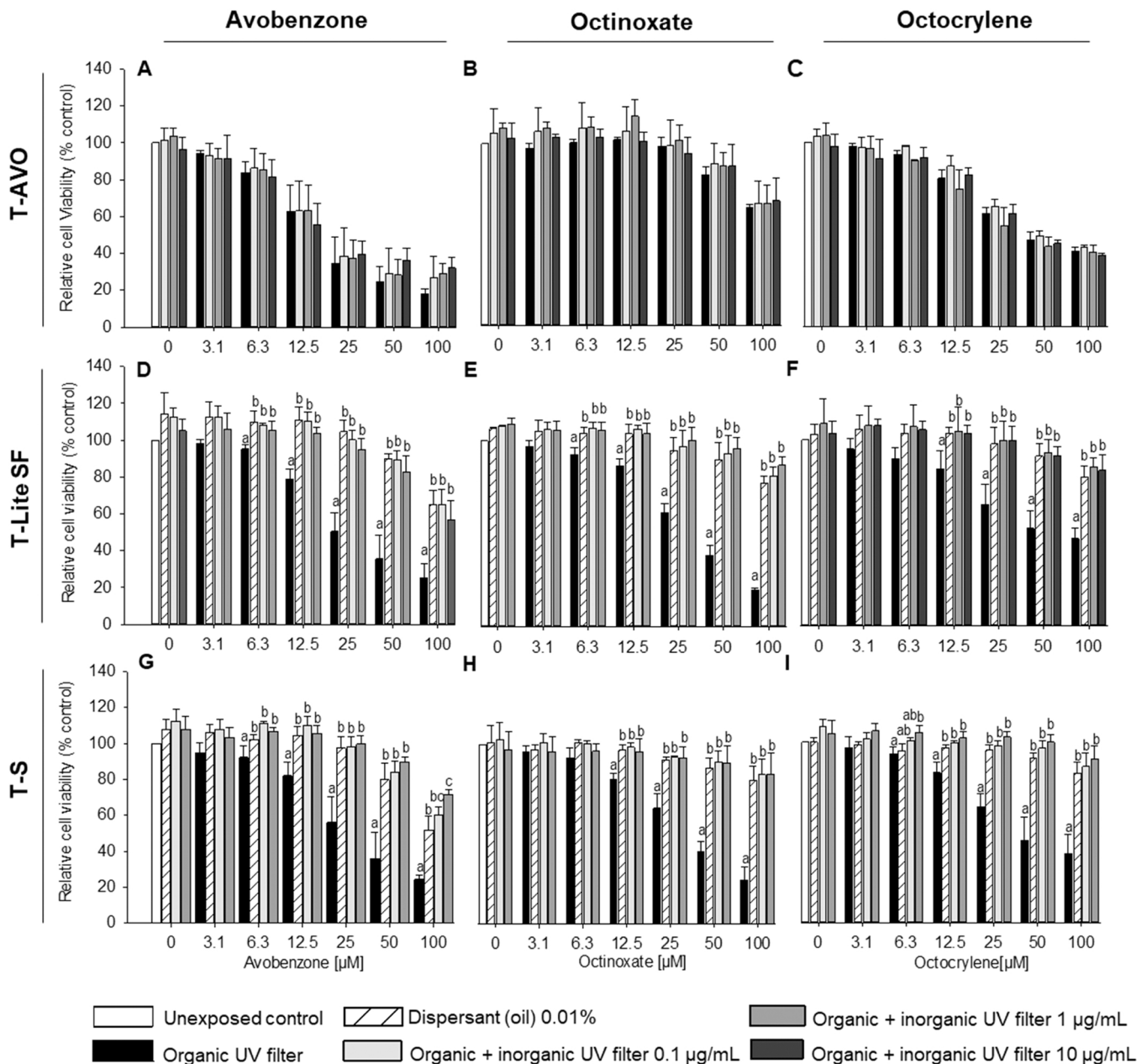


Fig. 5. Effects on RTgill-W1 cell viability following exposure to binary mixtures of TiO₂ NP UV filters and organic UV filters as determined by the NR assay. Bars and error bars show the mean and SD of three independent experimental replicates (n = 3). Letters above bars denote statistically significant differences between treatments with and without TiO₂ NPs (different concentrations) (One-way ANOVA followed by Holm-Sidak multiple comparison test, p < 0.05).

EVOM² Epithelial Voltohmmeter (World Precision Instruments). In addition, at day 21, lucifer yellow (LY) leakage across the RTgill-W1 cell sheet was measured, by filling the upper compartment with a 100 μM LY solution and measuring LY-dependent fluorescence in aliquots sampled from the bottom compartment after 60 min incubation at 19 °C. The relative amount of LY leakage was determined using a LY standard curve (=two-fold serial dilution of the 100 μM solution) included in the well plate, and measured at the same time.

2.5.2. TEM analysis of RTgill-W1 ThinCert cultures exposed to TiO₂ NP UV filters

RTgill-W1 cells cultured on ThinCerts (see 2.5.1) were exposed in duplicate to T-AVO, T-Lite SF, and T-S dispersions (10 μg/mL/μg/mL) for 24 h at 19 °C. Afterwards, the exposure medium was removed, and the cells were washed with Dulbecco’s PBS with Ca²⁺ and Mg²⁺, fixed in modified Karnovsky’s fixative, post-fixed in 1% osmium tetroxide

(OsO₄) including 1% potassium ferrocyanide, stained with 0.5% uranyl acetate, dehydrated in an ethanol gradient and then embedded in Agar 100 resin (Agar Scientific Ltd., UK). No post-staining was applied. Ultrathin sections (~70 nm) were collected on hexagonal 150 mesh copper grids and imaged on a Talos L120C (FEI, Thermo Scientific) equipped with a 4×4k CMOS Ceta camera. A similar amount of time was spent scanning the ultrathin sections originating from the different treatments (approximately 3 h; The sections were scanned until a representative overview of the samples was obtained, and the impression was gained that no new information would be attained by continuing analysis).

2.6. Study of effects of TiO₂ NP UV filters, organic UV filters, and binary mixtures on RTgill-W1 cell viability

Two experimental approaches were conducted to obtain information on the cytotoxicity of the UV filters and mixtures. The first approach,

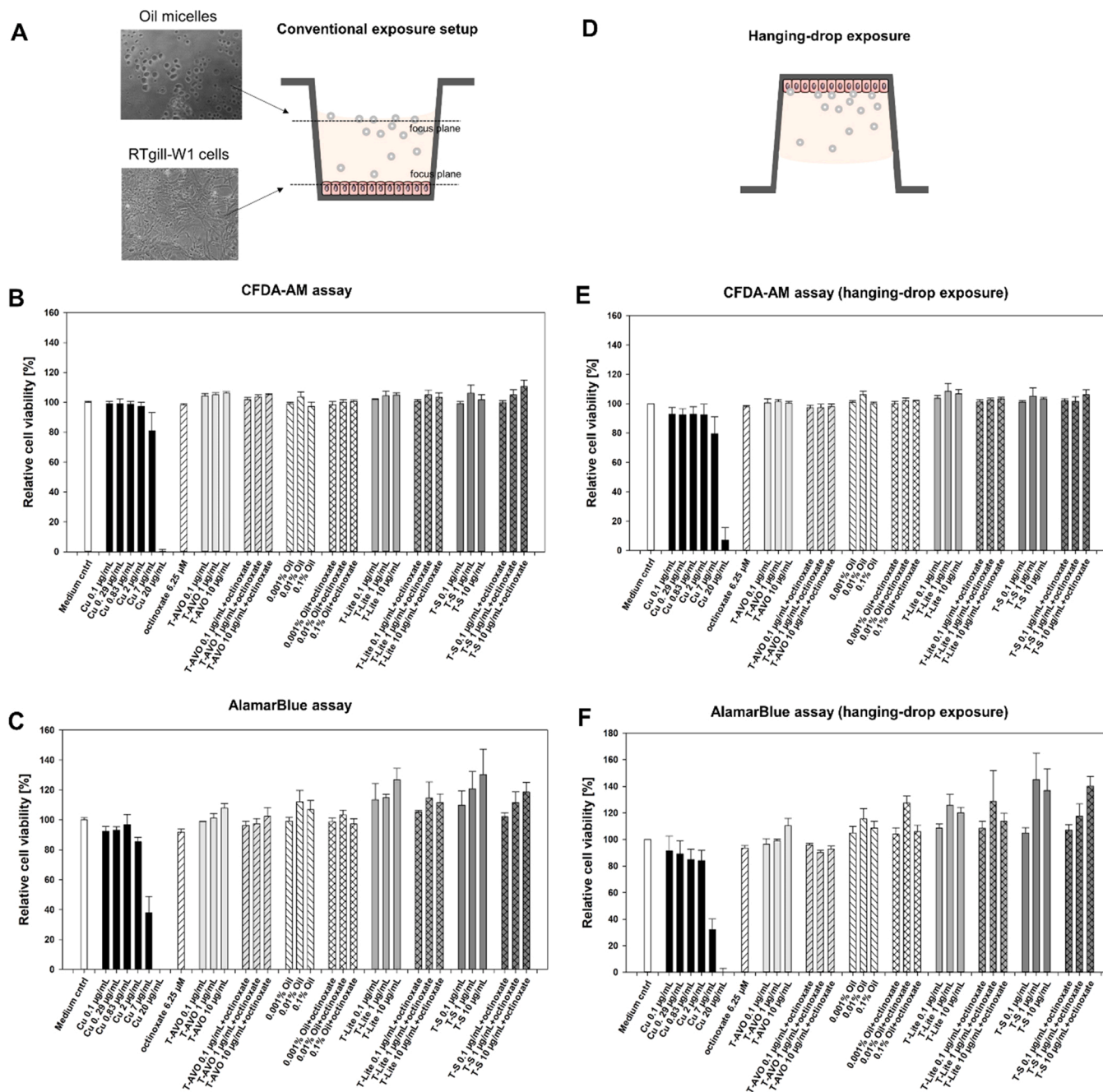


Fig. 6. Effect of water accommodated fractions of TiO₂ NP UV filters, organic UV filters, and mixtures on RTgill-W1 cell viability. **A.** Illustration of the conventional exposure setup. Bright-field microscopy images showing cells attached to the well bottom and oil droplets at the medium surface were taken at 100x magnification. **B** and **C.** CFDA-AM and AlamarBlue assay results obtained in the conventional exposure, respectively. **D.** Illustration of the hanging drop-exposure setup. **E** and **F.** CFDA-AM and AlamarBlue assay results obtained in the hanging drop-exposure, respectively. White bars: unexposed control (medium). Black bars: positive control (copper). Different shades of grey: Treatments containing T-AVO (light grey), T-Lite SF (grey), and T-S (dark grey). Ascending diagonal stripes: Treatments containing octinoxate. Descending diagonal stripes: treatments containing oil/emulsifier solution. Bars and error bars show the mean and SD of three experimental replicates. Statistical analysis (One way ANOVA) did not reveal any significant differences between treatment means.

described in Section 2.6.1., corresponded to standard procedures used for chemical toxicity testing (the substances were applied at a determined nominal concentration to the cells). The second approach, described in Section 2.6.2, aimed at testing the substances at more environmentally relevant conditions (exposure to water accommodated fractions).

2.6.1. Exposure to TiO₂ NP UV filters, organic UV filters, and mixtures

The NP stock dispersions (see above) were diluted in L15/ex medium to the concentrations used for cell exposure, that are, 0.1, 1 and 10 µg/

mL for T-AVO, and 0.1 and 1 µg/mL for T-S and T-Lite SF (note that the hydrophobic NPs were not tested at 10 µg/mL in order not to exceed 0.01% of oil solution in the exposure medium). The NP dispersions in L-15/ex were vigorously shaken by hand for one minute, and then sonicated for 60 s in pulse mode (1 s on /1 s off) using a Branson 250 sonifier equipped with a 3 mm diameter tapered microtip (Branson Ultrasonics Corporation, Danbury, Connecticut, USA) and operated at 10% maximum amplitude (~20 W). During sonication, the dispersions were kept in an ice-water bath. In parallel, L-15/ex containing 0.01% of the oil solution was prepared following the same protocol and used as

Table A1

Hydrodynamic size of T-AVO in L-15/ex as determined by DLS. The table shows the z-average (Z-Ave), polydispersity index (PdI), hydrodynamic diameter (mean \pm SD) and relative intensity (Int) of detected peaks (Pk; i.e., particle populations) at different concentrations (Conc.) and times (t₀, t = 24 h). * The difference between the Z-Ave and size of Pk1 is due to differences in the position and number of size peaks detected in the four consecutive measurements performed on the same sample (see Fig. S1). ** a second particle population with an average agglomerate size of 5252 \pm 449 nm and a relative peak intensity of 7% was observed in this sample.

Sample	Conc. (ug/mL)	Oil/Emul	t (h)	Z-Ave (d.nm)	PdI	Pk1 size (d.nm)	Pk1 Int (%)
T-AVO	0.1	No	0	* 716	0.77	195 \pm 20	100
T-AVO	1	No	0	459	0.37	** 381 \pm 12	* 93
T-AVO	10	No	0	750	0.30	637 \pm 139	100
T-AVO	0.1	No	24	* 1710	1.00	278 \pm 20	100
T-AVO	1	No	24	* 3819	1.00	132 \pm 10	100
T-AVO	10	No	24	1139	0.28	1188 \pm 312	100

solvent control, (or more accurately, as dispersant control). These NP dispersions were then used for cell exposure, or for the preparation of the binary mixtures with the organic UV filter substances (that is, avobenzone, octinoxate, and octocrylene). The mixtures were prepared as follows: first, a two-fold serial dilution of the organic UV filter stock solutions in L-15/ex containing a fixed concentration of T-AVO, T-Lite SF, or T-S (i.e., 0.1, 1 or 10 μ g/mL) was prepared. The organic UV filter concentrations in the resulting mixtures were 3.1, 6.3, 12.5, 25, 50, and 100 μ M (100 μ M of avobenzone, octinoxate, and octocrylene correspond to 31 μ g/mL, 29 μ g/mL, and 36 μ g/mL, respectively). A solvent control containing the NPs at 0.1, 1 or 10 μ g/mL and in addition 0.1% DMSO was included, too. Thereafter, the mixtures were incubated for two hours shielded from light at room temperature to allow the NPs to interact with the organic UV filters and establish chemical equilibrium (the dispersions/solutions containing only the NPs and only the organic UV filters were also incubated for two hours). Then, the dispersions/solutions were added in triplicate to microtiter plates (Sarstedt TC plate 96 well, standard, flat bottom) containing confluent RTgill-W1 cell

Table A2

Absorbance and transmittance of monochromatic light (wavelengths used in cell viability assay) by NP residues retained in well/cell cultures exposed to TiO₂ NP UV filters T-AVO, T-LITE SF, and T-S. Absorbance measurements were conducted after washing with L-15/ex (2x). The stated concentrations (0.1, 1, and 10 μ g/mL) are the applied nominal concentrations. All shown absorbance values multiplied by 1000 (A) are blank-corrected, including those obtained for wells exposed to only L-15/ex (unexposed control) and wells exposed to 0.01% oil solution but no NPs (Oil). Transmittance values (T) were calculated from A using the following formula: $100 \cdot 10^{-A}$. All values correspond to the mean and SD of three independent experimental replicates (n = 3).

λ [nm]	μg/mL	360		450		485		535		595		645	
		A	T	A	T	A	T	A	T	A	T	A	T
T-AVO	10	56 \pm 7.4	89.3 \pm 1.0	32.0 \pm 2.0	93.0 \pm 0.6	27.9 \pm 1.2	94.0 \pm 0.5	23.1 \pm 0.6	95.0 \pm 0.4	16.4 \pm 1.3	96.6 \pm 0.4	18.7 \pm 0.6	96.0 \pm 0.4
	1	12.0 \pm 7.3	98.3 \pm 1.1	6.1 \pm 3.5	98.5 \pm 0.7	5.0 \pm 3.4	98.7 \pm 0.6	4.5 \pm 2.2	98.9 \pm 0.5	3.2 \pm 1.4	99.3 \pm 0.4	3.8 \pm 1.6	99.2 \pm 0.4
	0.1	2.7 \pm 7.3	100.0 \pm 0.9	2.8 \pm 2.9	99.0 \pm 0.5	2.5 \pm 2.7	99.1 \pm 0.4	2.4 \pm 1.7	99.2 \pm 0.3	1.8 \pm 0.8	99.5 \pm 0.2	2.1 \pm 1.2	99.4 \pm 0.3
T-Lite SF	1	12.3 \pm 5.4	97.2 \pm 1.2	10.3 \pm 4.9	97.7 \pm 1.1	9.9 \pm 4.9	97.7 \pm 1.1	8.0 \pm 3.7	98.2 \pm 0.8	5.7 \pm 2.9	98.7 \pm 0.7	6.8 \pm 3.6	98.4 \pm 0.8
	0.1	10.8 \pm 0.7	97.5 \pm 0.2	9.4 \pm 1.9	97.9 \pm 0.4	8.7 \pm 1.6	98.0 \pm 0.4	7.7 \pm 1.1	98.3 \pm 0.3	5.4 \pm 1.2	98.8 \pm 0.3	7.2 \pm 0.2	98.4 \pm 0.0
T-S	1	16.5 \pm 3.0	96.3 \pm 0.7	12.9 \pm 3.1	97.1 \pm 0.7	11.5 \pm 2.7	97.4 \pm 0.6	9.9 \pm 2.3	97.7 \pm 0.5	7.6 \pm 1.9	98.3 \pm 0.4	8.6 \pm 2.2	98.0 \pm 0.5
	0.1	13.4 \pm 6.9	97.0 \pm 1.5	12.3 \pm 5.5	97.2 \pm 1.2	11.2 \pm 5.3	97.5 \pm 1.2	9.5 \pm 4.6	97.8 \pm 1.0	7.4 \pm 3.5	98.3 \pm 0.8	8.3 \pm 3.8	98.1 \pm 0.9
Oil	-	6.8 \pm 2.8	98.4 \pm 0.6	7.5 \pm 2.6	98.3 \pm 0.6	7.0 \pm 2.2	98.4 \pm 0.5	6.0 \pm 2.1	98.6 \pm 0.5	4.3 \pm 1.8	99.0 \pm 0.4	5.2 \pm 1.9	98.8 \pm 0.4
Unexposed	-	5.9 \pm 10.8	100 \pm 0.7	2.8 \pm 1.5	99.3 \pm 0.3	2.2 \pm 1.6	99.4 \pm 0.3	1.8 \pm 1.2	99.5 \pm 0.2	1.3 \pm 1.0	98.8 \pm 0.2	1.6 \pm 0.9	99.7 \pm 0.2

monolayer cultures (50,000 cells per well) seeded the day before. The volume added to each well was 100 μ l. The exposed well plates were incubated for 24 h at 19 °C in the dark, and then rinsed twice with L-15/ex, and analysed using the AlamarBlue, CFDA-AM and NR assays described below. The entire experiment was repeated at least three times, on different days, using freshly prepared solutions/dispersions.

2.6.2. Exposure to water accommodated fractions of TiO₂ NP UV filters, organic UV filters, and binary mixtures

In this study, we decided to conduct an additional set of experiments employing an alternative experimental approach than the one usually used in cytotoxicity testing/screening of NPs. In this approach, the dispersions prepared in L-15/ex were first placed on an orbital shaker for 48 h, and thereafter samples were taken from the centre of the vial and applied to the cells. This approach was chosen to test the effect of only that particle population (and organic co-pollutant) which is expected to remain stably suspended in the water column (L-15/ex is a saline solution with an ionic strength 173 mM, which apart from galactose and pyruvate that are needed as an energy source does not contain any other of the typical cell culture medium ingredients such as amino acids, vitamins and, serum proteins. Thus, even though the ionic composition differs, L-15/ex can be considered to simulate to some extent brackish-water environments). The methodological details were as follows.

On day 1, T-AVO was dispersed in Milli-Q water at 10 mg/mL. T-Lite SF and T-S were dispersed in oil at 10 mg/mL. The NP dispersions were diluted to the experimental concentrations of 10, 1 and 0.1 μ g/mL in L15/ex solution with 0.1% DMSO or 6.25 μ M octinoxate. The octinoxate concentration was selected as it was among the lowest concentrations that exhibited a clear decrease in cell viability in the range finding test (Figure 10). In addition, solutions serving as the negative control (only L-15/ex solution), solvent controls (0.1%, 0.01% and 0.001% oil incl. DMSO) and only-octinoxate control were prepared. The dispersion/solution-containing glass vials were placed on a shaker set to 450 rpm and incubated for 48 h while shielded from light.

On day 2, gill cells were seeded in 96-well plates (Sarstedt) at 50,000 cells per well (Volume per well: 100 μ l; Medium: L-15 with 5% FBS; Passage number 25) and placed in an incubator set to 19 °C to allow cell attachment and formation of a confluent monolayer.

On day 3, the shaker was stopped and after ~30 min 100 μ l aliquots were sampled from the middle of the glass vials containing the WAF and

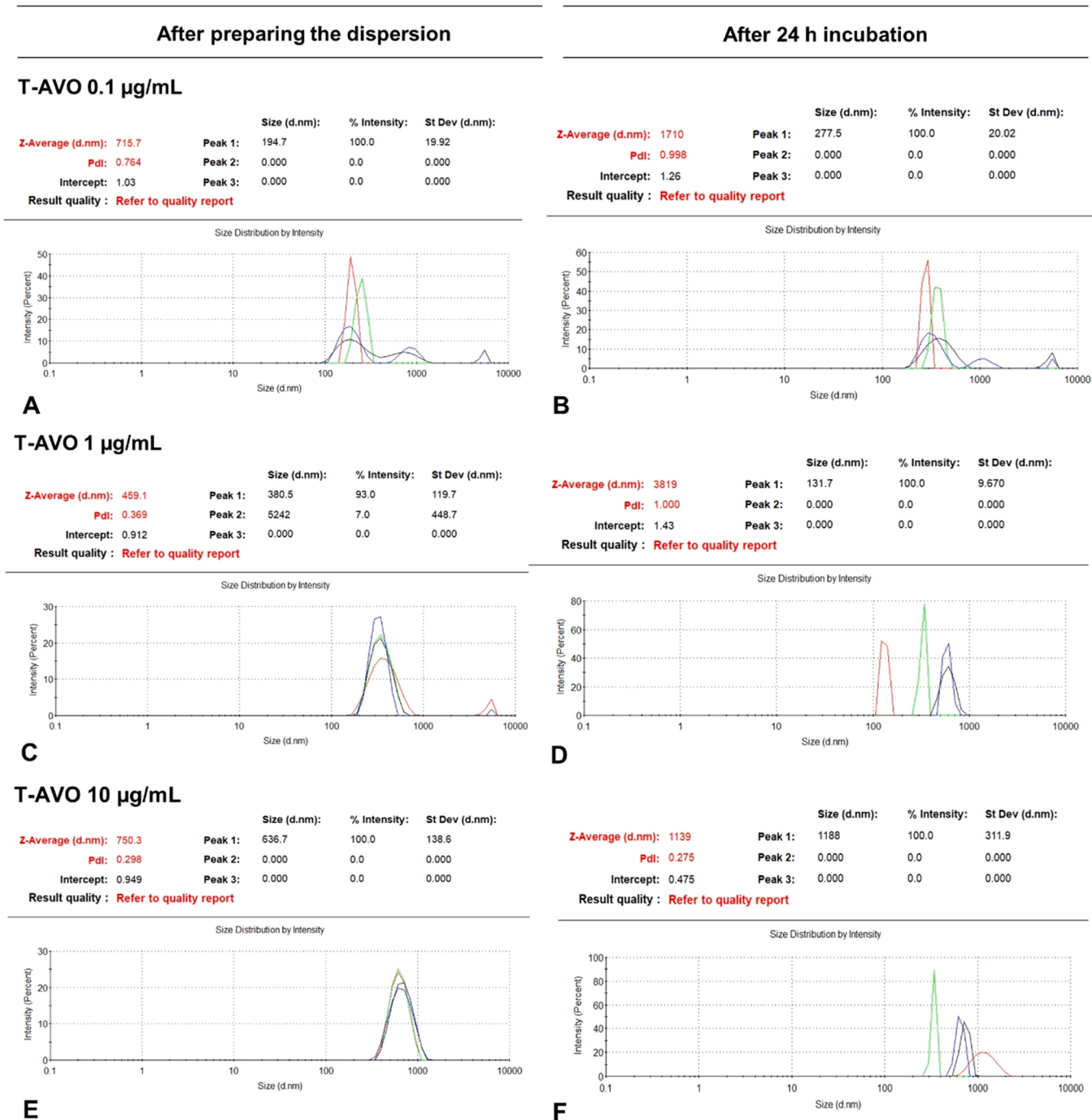


Fig. A1. Particle size distribution by intensity of T-AVO in L-15/ex as determined by DLS. Peaks with different colours correspond to separate measurements. Graphs on the left (A, C, and E) show the particle size distribution at t0, graphs on the right (B, D, and F) show the particle size distribution after 24 h. The graphs in the top (A, B), middle (C, D) and bottom (E, F) of the figure correspond to the lowest, intermediate and highest NP concentration tested, that is 0.1, 1, and 10 µg/mL, respectively. In addition, above each graph, the intensity weighted harmonic mean size (Z-average) and polydispersity index (Pdl), as well as the particle diameter in nanometres (d.nm) of the predominant particle populations (peaks) are displayed (together with their relative intensity of the later).

applied to RTgill-W1 cell cultures. Treatments were applied in triplicate (three wells). For each plate a duplicate plate was prepared, which was carefully turned upside-down for “hanging drop” exposure (see Fig. 6D). The purpose of this exposure was to have an additional control that accounts for the possibility that hydrophobic TiO₂ NP UV filters or NP-oil micelles would raise to the medium surface and not “reach” the cells in the conventional exposure setup. All plates were sealed with parafilm and incubated at 19 °C for 24 h in the dark, and thereafter analysed using the CFDA-AM and AlamarBlue assays (described below). As previously discussed (see above), a hanging drop exposure was conducted

in parallel, where the (same) WAFs were pipetted on top of cell monolayers cultured in 96-well plates, but the well plates were then incubated upside-down (cp. illustrations in Fig. 6 A and D).

2.7. Cell viability assays

Cell viability was determined by three fluorescence-based assays that measure impairment of different cellular structures/functions: The CFDA-AM assay measures the intracellular esterase activity providing information on plasma membrane integrity/damage, the alamarBlue

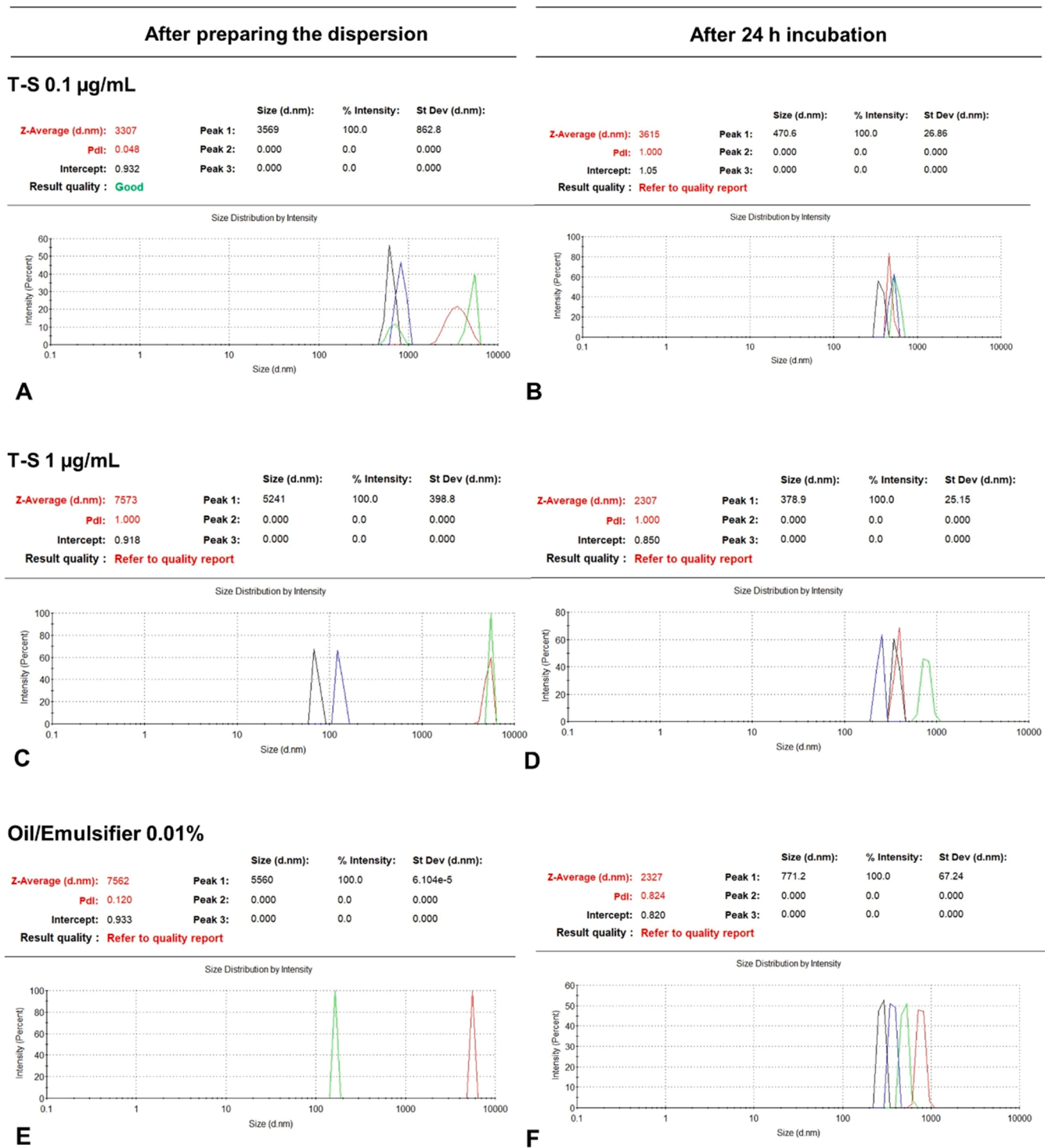


Fig. A2. Particle size distribution by intensity of T-S in L-15/ex as determined by DLS. Peaks with different colours correspond to separate measurements. Graphs on the left (A, C, and E) show the particle size distribution at t0, graphs on the right (B, D, and F) show the particle size distribution after 24 h. The graphs in the top (A, B) and the middle (C, D) correspond to the two NP concentrations tested, that is 0.1, and 1 µg/mL, respectively. The graphs in the bottom of the figure (E, F) show the peaks detected for only the oil/emulsifier solution. In addition, above each graph, the intensity weighted harmonic mean size (Z-average) and polydispersity index (Pdl), as well as the particle diameter in nanometres (d.nm) of the predominant particle populations (peaks) are displayed (together with their relative intensity of the later).

assay measures the intracellular redox state providing information on cellular metabolic activity, and the Neutral Red (NR) assay measures accumulation of NR in lysosomes providing information about their structural and functional integrity (Bols et al., 2005). AlamarBlue and CFDA-AM can be applied together (i.e., as one solution), and the NR dye

can be applied afterwards on the same set of cells. The assays were carried out as described by (Dayeh et al., 2003) with some modifications specified below.

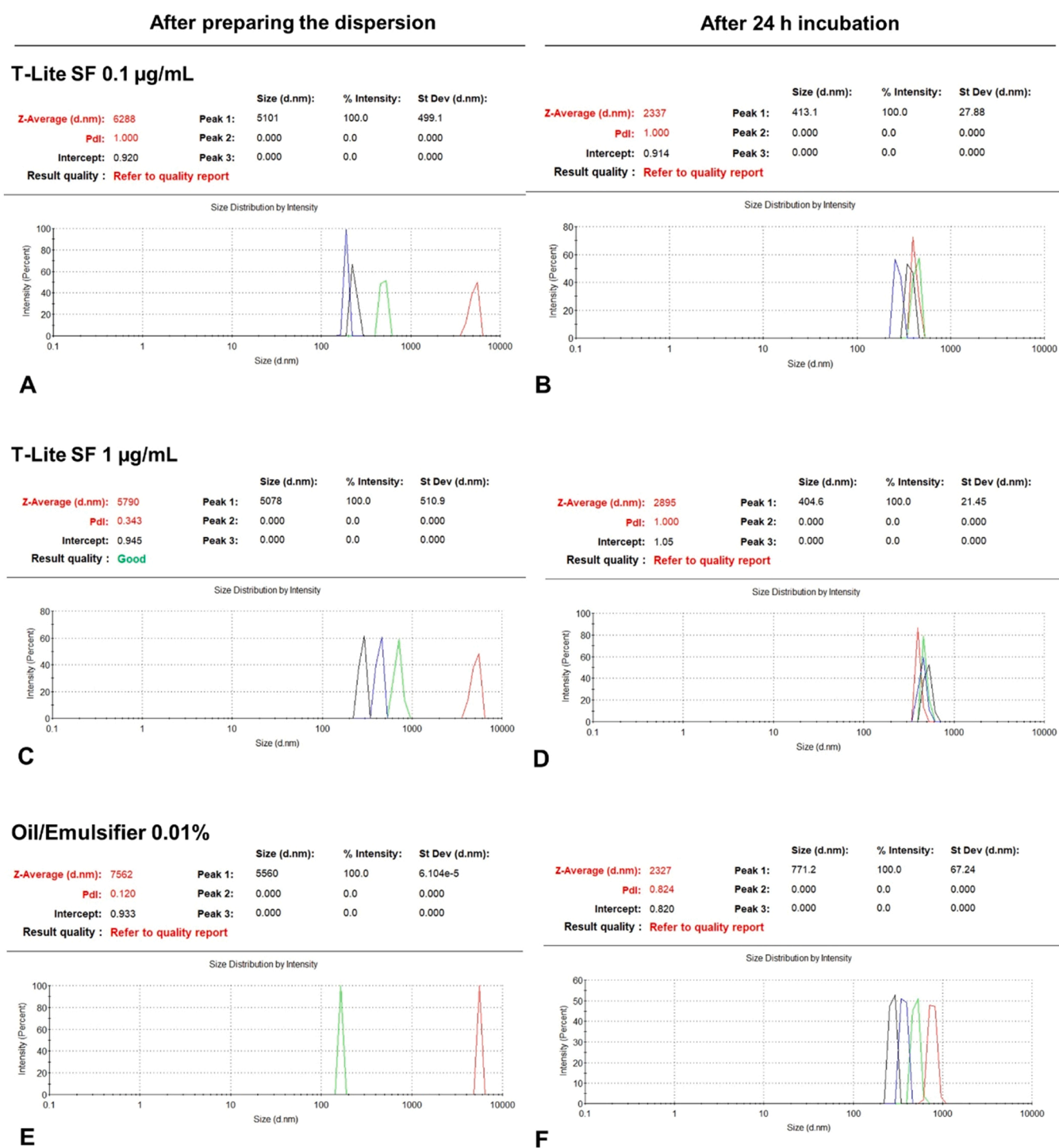


Fig. A3. Particle size distribution by intensity of T-Lite SF in L-15/ex as determined by DLS. Peaks with different colours correspond to separate measurements. Graphs on the left (A, C, and E) show the particle size distribution at t0, graphs on the right (B, D, and F) show the particle size distribution after 24 h. The graphs in the top (A, B) and the middle (C, D) correspond to the two NP concentrations tested, that is 0.1, and 1 µg/mL, respectively. The graphs in the bottom of the figure (E, F) show the peaks detected for only the oil/emulsifier solution. In addition, above each graph, the intensity weighted harmonic mean size (Z-average) and polydispersity index (Pdl), as well as the particle diameter in nanometres (d.nm) of the predominant particle populations (peaks) are displayed (together with their relative intensity of the later).

2.7.1. Standard assay protocol

After removal of the exposure solutions/dispersions and rinsing the cells with L-15/ex, 100 µl of AlamarBlue/CFDA-AM solution (1.25% of AlamarBlue solution and 4 µM CFDA-AM dissolved together in L15/ex) were added to each well, and the well plates were incubated at 19 °C for 30 min. Thereafter, the fluorescence intensity was measured at

excitation/emission wavelengths of 532/590 nm (AlamarBlue assay) and 485/535 nm (CFDA-AM assay) using a SpectraMax Gemini EM microplate reader (Molecular Devices). After fluorescence readout, the AlamarBlue/CFDA-AM solution was removed, the cells carefully washed once with 150 µl L-15/ex and then incubated with 100 µl of L-15/ex containing 10% of a 0.33% commercial Neutral Red solution for one

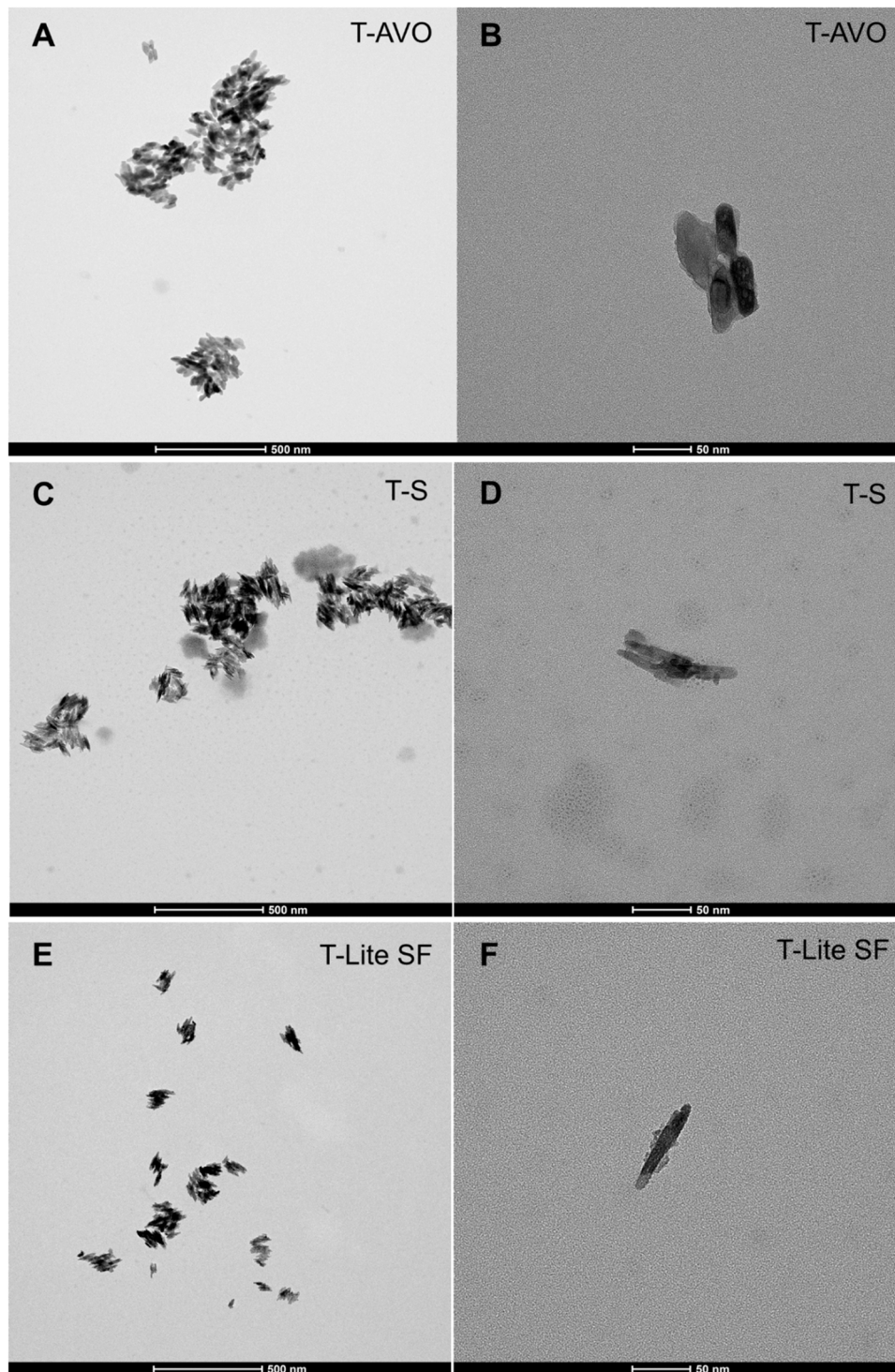


Fig. A4. TEM images of TiO_2 NP UV filters after dilution in L-15/ex. A and B: T-AVO (10 $\mu\text{g}/\text{mL}$), C and D: T-S (10 $\mu\text{g}/\text{mL}$), E and F: T-Lite SF (10 $\mu\text{g}/\text{mL}$). Scale bars in A, C and E correspond to 500 nm, scale bars in B, D and F correspond to 50 nm.

more hour at 19 °C in the dark. Then, following three washing steps with 150 μl of L-15/ex, 100 μl of destaining solution (50% ethanol and 1% glacial acetic acid diluted in deionized water) were added per well, the plates were agitated for 30 s, and incubated for another 10 min 19 °C in the dark. Subsequently, NR fluorescence intensity was measured at excitation/emission wavelengths of 630/645 nm using the microplate reader specified above. Relative cell viability was calculated as follows: The fluorescence intensities from the endpoint measurement were corrected for background fluorescence by subtracting the values measured

in the cell-free control (blank), and thereafter expressed as percentage of the fluorescence intensity measured in the unexposed control.

To estimate interference by TiO_2 NP UV filter residues retained in the well plate through attenuation of light at the wavelengths used for excitation or recording emission in the cell viability assays, additional absorbance measurements at 360, 450, 485, 535, 595, and 645 nm were performed on each 96-well plate. Absorbance measurements were done after removal of the exposure solutions/dispersion and washing cells with L-15/ex, but before addition of the AlamarBlue/CFDA-AM

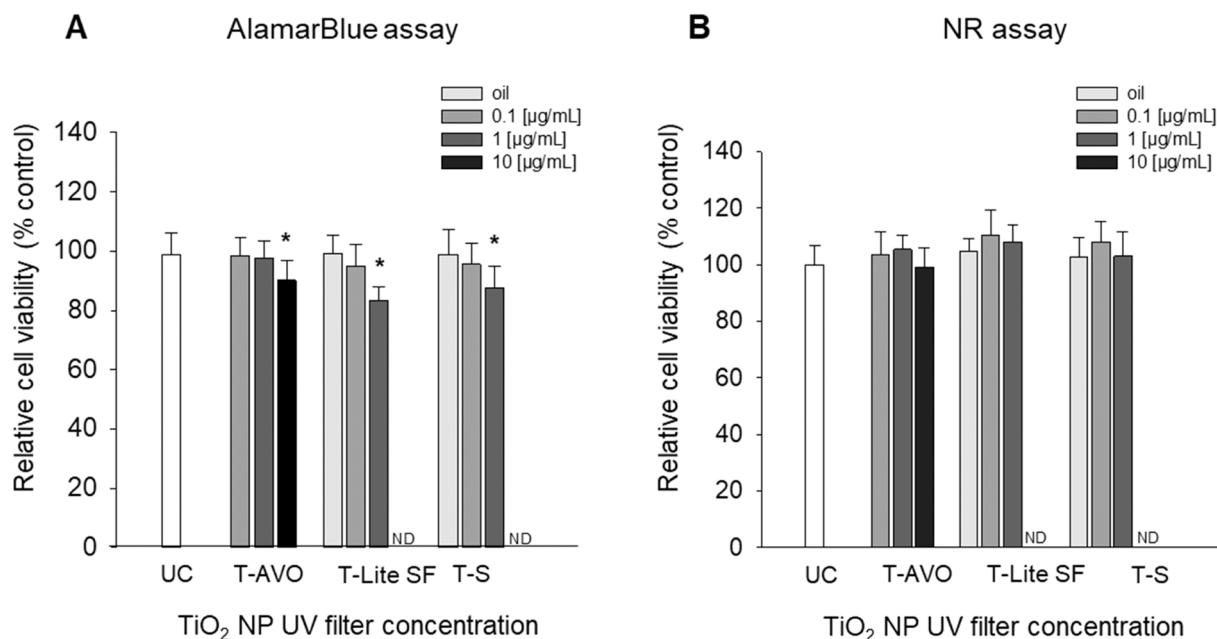


Fig. A5. Effect of the TiO₂ NP UV filters T-AVO, T-Lite SF and T-S on RTgill-W1 cell viability as determined by the AlamarBlue assay (A) and the NR assay (B). Results obtained using the standard protocol (endpoint analysis). Bars and error bars show means and SD of nine independent experimental replicates (n = 9). Asterisks (*) indicate statistically significant differences (p < 0.05) compared to the unexposed control (one way ANOVA followed by Holm-Sidak). Note that the highest exposure concentration of T-Lite SF and T-S was 1 µg/mL (the “missing” 10 µg/mL treatments are indicated as ND = not determined).

solution, using a SpectraMAx® 190 absorbance plate reader.

2.7.2. Modified assay protocol (kinetic analysis)

In addition to the endpoint measurements described above, the 96-well plates were analysed using a modified protocol of the CFDA-AM assay, where fluorescence intensity was recorded over time, and the slopes of a linear regression model fitted over the fluorescence intensity curve used to calculate relative cell viability, as follows:

$$\text{Relative cell viability } [\%] = \frac{\text{slope (treatment)} - \text{slope (blank)}}{\text{slope (unexposed control)} - \text{slope (blank)}} \times 100$$

2.8. Statistical analysis

Statistical comparisons of different groups were performed using One-way analysis of variance (One-way ANOVA) followed by the Holm-Sidak method. All data were tested for normality (Shapiro-Wilk test) and equal variance (Brown-Forsythe test) prior to One-way ANOVA. The significance level in all tests below which the null hypothesis (= group means are not different from each other) was rejected was p = 0.05. Data that failed to pass either the Shapiro-Wilk or Brown-Forsythe test and hence did not meet the criteria to be analysed using a parametric test were analysed with a Kruskal-Wallis One Way ANOVA on Ranks instead. Half maximum effect concentrations (EC50) were estimated from dose-response curves fitted over the measurement data using a three-parameter sigmoid regression model. All data analysis was performed using SigmaPlot for Windows version 14 (Systat Software Inc.).

3. Results and discussion

3.1. NP size and behaviour in L-15/ex medium

DLS analysis revealed that the SiO₂-coated TiO₂ NP UV filter T-AVO was mainly present in form of agglomerates in L-15/ex medium, and that agglomerate size was larger in the higher concentrated samples (0.1 µg/mL: 195 ± 20 nm, 1 µg/mL: 381 ± 120 nm, 10 µg/mL: 637 nm

± 139 nm). NP agglomeration proceeded, and was possibly accompanied by sedimentation of larger agglomerates, but overall the particle size distribution appeared to be fairly stable over the 24 h measurement period (i.e., the exposure time) (Table A1, Fig. A1). The zeta-potential of T-AVO in L-15/ex was −19 mV, which is consistent with the observation that its colloidal stability was good but limited. The zeta-potential corresponds well to that measured for SiO₂ NPs in L-15/ex (Book et al., 2019), that is, the SiO₂-coating of T-AVO seemed to be intact.

The hydrodynamic size and zeta-potential of the hydrophobic TiO₂ NP UV filters T-Lite SF and T-S in L-15/ex could not be reliably determined by DLS. The position of the intensity peaks, being indicative of the size of the detected particle populations, differed considerably between repeated measurements performed on the same sample. The mean size of the detected particle populations ranged from several hundred to several thousand nanometres, indicating that T-Lite SF and T-S were probably present as agglomerates, and/or associated with oil micelles in these samples (Note: In the vehicle control, that is, L-15/ex containing 0.01% oil solution but no NPs, intensity peaks within the same range were observed) (Fig. A2 and A3). Furthermore, the attenuator index, automatically set by the instrument to adjust the laser power to scattering intensity, increased from 7 at t₀ to 11 at t = 24 h. This indicates a decrease in the particle concentration in the path of the laser beam, which can be explained by either gravitational settling of NP agglomerates and/or oil micelles rising to the surface of the water column during the incubation time. Overall, the DLS data show that it is likely, that in the case of T-Lite SF and T-S, the to-cell-delivered dose differed from the nominal exposure dose, possibly not during the first minutes but certainly toward the end of the exposure. TEM analysis confirmed the presence of large agglomerates in all three NP dispersions but also revealed the presence of smaller agglomerates (<100 nm) and individual NPs (Fig. A4), which were not visible in the DLS results, possibly because the light scattered by them was masked by the higher scattering intensity of the larger NP agglomerates.

3.2. Uptake of TiO₂ NP UV filters by RTgill-W1 cells

In this study, we intended to examine cellular uptake and

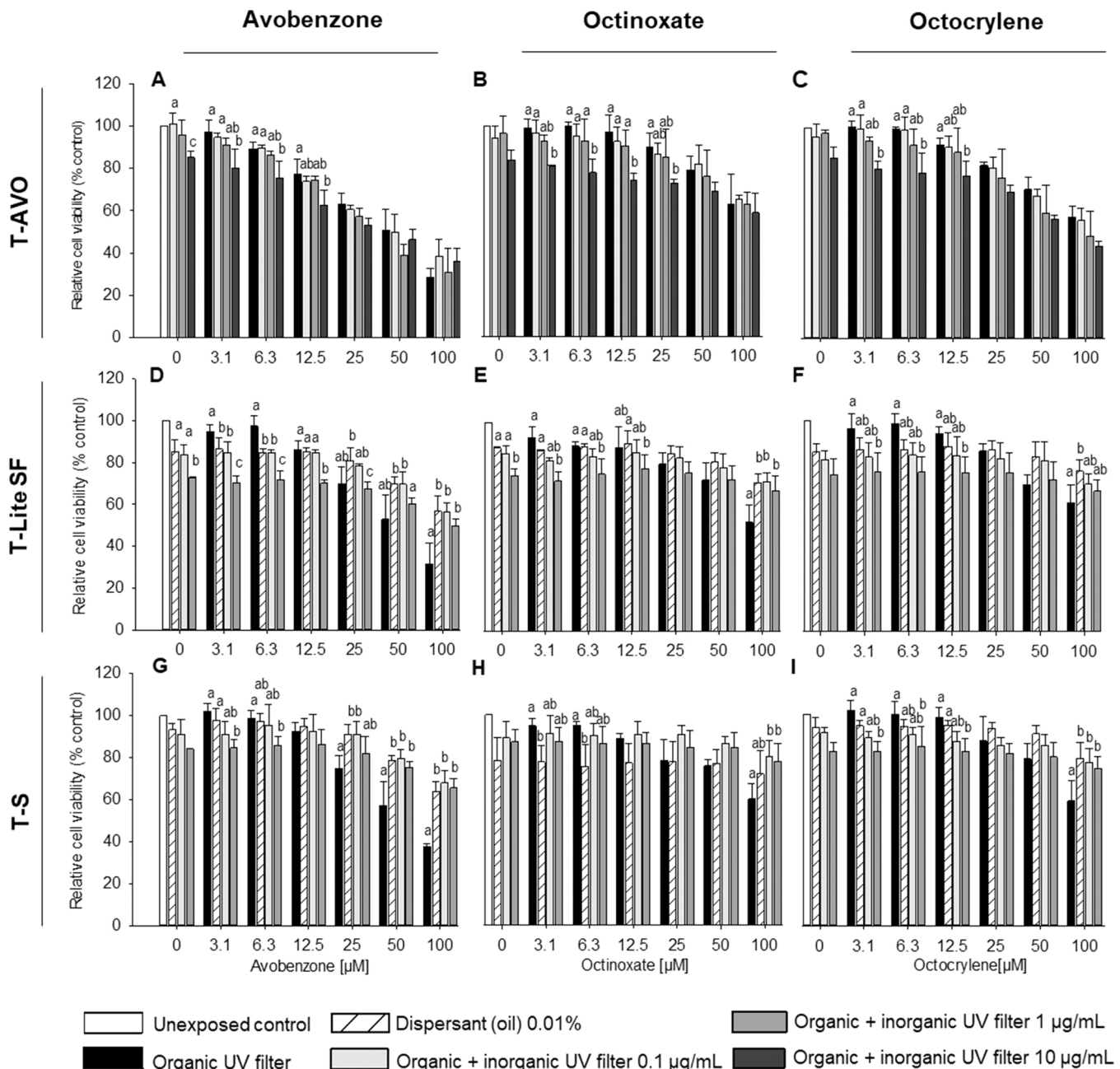


Fig. A6. Effects on RTgill-W1 cell viability following exposure to binary mixtures of TiO₂ NP UV filters and organic UV filters as determined by the CFDA-AM assay (endpoint analysis). Bars and error bars show the mean and SD of three independent experimental replicates (n = 3). Letters above bars denote statistically significant differences between treatments with and without TiO₂ NPs (different concentrations) (One-way ANOVA followed by Holm-Sidak multiple comparison test, p < 0.05).

translocation of TiO₂ NP UV filters across the gill epithelium using RTgill-W1 transwell cultures as an in vitro model. However, the TEER of RTgill-W1 cell monolayer cultures grown in Thincerts® for three weeks increased by only 23.6 ± 2.1 Ω cm² compared to t₀, and by only ~13 Ω cm² when compared to the TEER value in empty well-controls incubated for the same time, which was 12.2 ± 2.0 Ω cm². These values are in the range of those reported by Trubitt et al. (2015) and Mandal et al. (2020) (the maximum TEER in both studies was around 40 Ω cm²). However, compared to TEER values that are obtained for in vitro epithelial models developed from primary gill cells (TEER > 1000 Ω cm²) (Schnell et al., 2016), these values are very low, indicating that RTgill-W1 Thincert® cultures did not form an electrically tight epithelium. Furthermore, LY leakage across the RTgill-W1 cell layer, which was ~4.5% within 60 min, exceeded the threshold value below

which in vitro epithelial barrier integrity is considered appropriate (i.e., tight enough) for permeability/translocation studies (typically <2–3%, depending on the cell line and manufacturer guideline). Therefore, in this study, we refrained from examining NP translocation across the RTgill-W1 cell layer using quantitative methods, such as inductively coupled plasma mass spectrometry (ICP-MS), and used the Thincert® cell cultures instead to (only) investigate cellular uptake (i.e., internalisation) of the TiO₂ NP UV filters using TEM.

TEM analysis revealed that T-AVO was the only one of the three tested TiO₂ NP UV filters that was taken up by RTgill-W1 cells (Fig. 1). T-AVO NPs were present in the form of agglomerates of varying sizes (comparable to those imaged in the dispersion used for exposures, see Fig. A4), and were located inside intracellular vacuoles with multiple, concentrically-arranged membranes (Fig. 1A and B). Previous

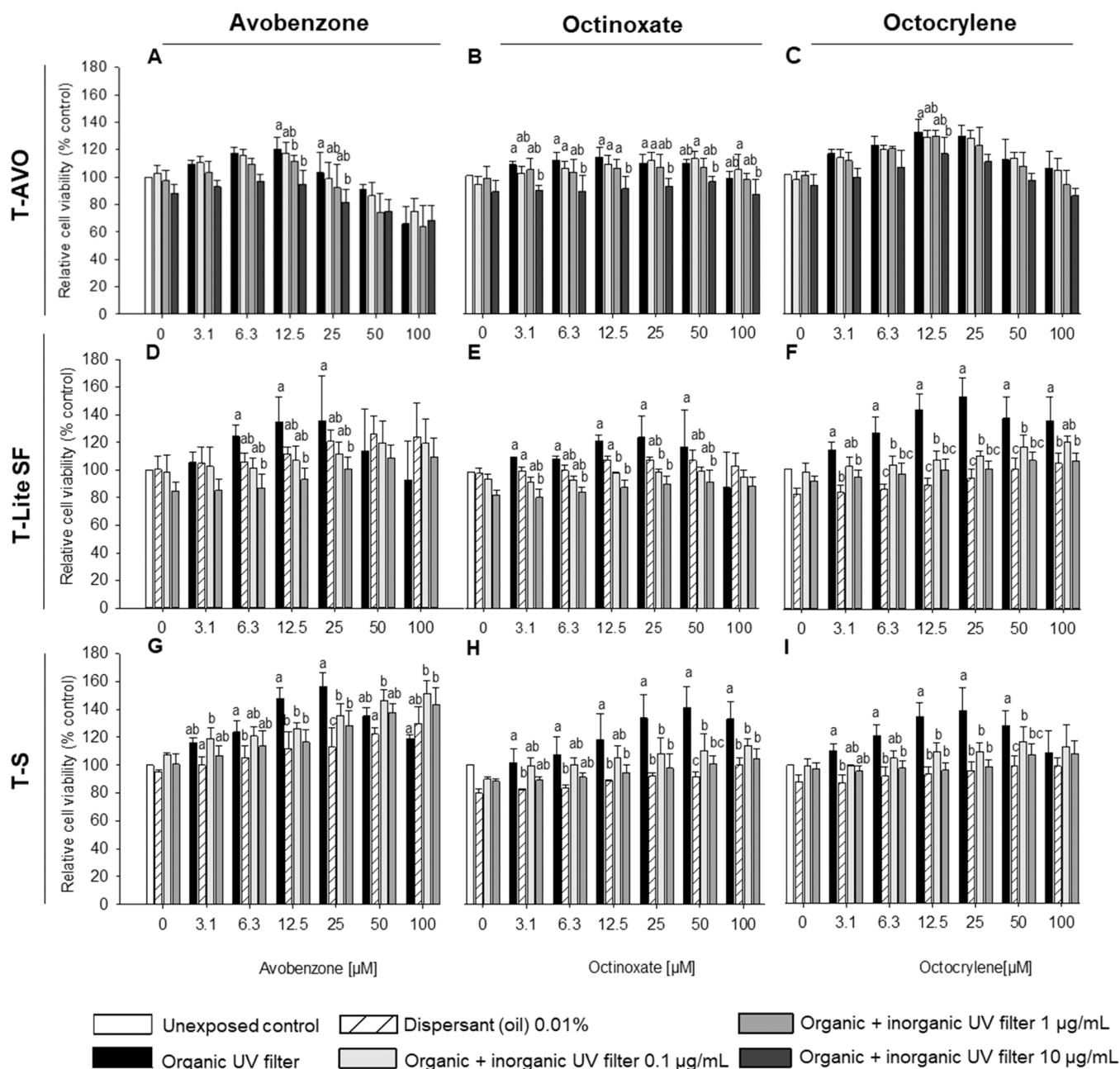


Fig. A7. Effects on RTgill-W1 cell viability following exposure to binary mixtures of TiO₂ NP UV filters and organic UV filters as determined by the AlamarBlue assay. Bars and error bars show the mean and SD of three independent experimental replicates (n = 3). Letters above bars denote statistically significant differences between treatments with and without TiO₂ NPs (different concentrations) (One-way ANOVA followed by Holm-Sidak multiple comparison test, p < 0.05).

observation of this phenomenon in different cell types and for other nanomaterials (e.g., in rainbow trout liver cells exposed to TiO₂ P25) (Lammel et al., 2019a; Lammel and Sturve, 2018), makes us hypothesize that the formation of several membrane layers around the internalised NPs may represent an unspecific adaptive response aiming at isolating the foreign material to prevent potential cell damage.

TEM images of RTgill-W1 cells exposed to T-Lite SF and T-S, on the contrary, did not provide any evidence for NP internalisation (Fig. 1C and D, respectively). T-Lite SF and T-S differ from T-AVO by having a hydrophobic instead of a hydrophilic coating (PDMS and stearic acid, respectively). Therefore, our results suggest that the surface chemistry of TiO₂ NP UV filters has a critical influence on their interaction and uptake by cells. However, it is important to bear in mind that the total to-cell-delivered dose of T-Lite SF and T-S was probably lower (compared to T-AVO) because of their entrapment in oil droplets (see 3.1. for

discussion), and other factors such as agglomerate size may affect uptake efficiency as well (Lammel et al., 2019a; Zhao and Stenzel, 2018).

3.3. Cytotoxicity of TiO₂ UV NP filters compared to organic UV filters

Mineral UV filters are believed to pose a lower hazard to aquatic life than organic UV-filters. In this study, we measured and compared the cytotoxicity of three different TiO₂ NP UV-filters (T-AVO, T-Lite SF and T-S) and three organic chemical UV-filters commonly used in sunscreens (avobenzone, octinoxate, and octocrylene) in RTgill-W1 cells, using fluorescence-based assays focussing on different cellular endpoints (modes of action): plasma membrane integrity/damage, cellular metabolic activity, and lysosomal integrity (cp. Section 2.7.). Effects on the latter endpoint were of particular interest, as lysosomal NP uptake and damage has been proposed as a key event involved in nanomaterial

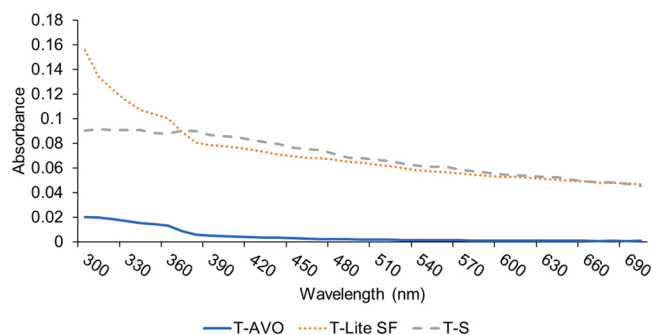


Fig. A8. Absorbance spectrum of tested TiO₂ NP UV filters measured each 10 nm on the UV–visible wavelength range containing excitation and emission wavelength of fluorophores used in cell viability assays. Measurements were conducted in 100 μ l of L15/ex with 1 μ g/mL of NPs with 0.01% of oil/emulsiifier for T-Lite SF and T-S. Absorbance values are blank corrected with L15/ex solution.

toxicity (Gerloff et al., 2017; Stern et al., 2012).

The obtained results show that none of the tested TiO₂ UV filters (including T-AVO which was taken up by the cells) had any significant effect on these endpoints in the conditions of this study (Figs. 2, 5). An apparent reduction in cell viability was observed when applied at high concentrations (1–10 μ g/mL), but control experiments indicated that this reduction was partly due to NP interference with the assay by absorption, scattering or reflection of the incident and or emitted light during fluorescence readout. Besides their characteristic absorbance peak in the UV range, all three TiO₂ NP UV filters absorbed light at the excitation and emission wavelengths used in the different assays (Fig. A8). Attenuation of transmittance was wavelength-dependent (being lower at the longer wavelengths), and the level of interference differed between assays, in the order: CFDA-AM > AlamarBlue > NR (Table A2, Fig. A9), which corresponds to our previous findings for TiO₂ P25 (Lammel and Sturve, 2018). Although the interference is minimal, it can confound results. For example, it may lead to misinterpretations when comparing effects caused by different types of NPs (when these cause different levels of interference) and or when comparing effects of treatments containing NPs with those without (i.e., NP-chemical mixtures with chemical only treatments). Therefore, in addition to including appropriate controls, strategies to avoid or deal with interference-issues need to be developed.

We tested if it was possible to obtain a more accurate estimate by performing a kinetic measurement instead of an endpoint measurement, and calculate the relative cell viability by comparing the slopes derived from a linear regression model fitted over the fluorescence intensity curve obtained for NP-exposed cell cultures and unexposed cell cultures (medium control). In contrast to the absolute fluorescence intensity values, the slopes should be unaffected by NP-caused absorption/scattering/reflection of the incident light used for excitation. The results obtained using this modified assay protocol did not show any effect by either of the NPs (compared to the unexposed control), supporting our hypothesis that the decrease in fluorescence intensity observed using the original protocol was owed to NP-interference (Fig. 2B, cp. with Fig. 2A). Although further validation with other NPs is needed, we believe that the modified protocol could be a possible approach to more accurately estimate the cytotoxicity of NPs that are likely to interfere with fluorescence-based assays because of their optical properties.

All tested organic UV filters showed a noticeable effect on RTgill-W1 cell viability within the tested concentration range (3.1 – 100 μ M) (Fig. 3). In the CFDA-AM assay and the NR assay, a decrease in cell viability with increasing exposure concentrations was observed, and the dose-response curve followed a sigmoid function (Fig. 3A and C). The NR assay was slightly more sensitive than the CFDA-AM assay, possibly because loosely attached cells were removed during the additional

washing steps of the NR protocol. The lowest observed effect concentrations (LOEC) and the half maximal effect concentrations (EC50) determined for avobenzone, octinoxate and octocrylene based on the NR assay data are shown in Table 1. Avobenzone was slightly more toxic to fish gill cells than octinoxate and octocrylene, which could be due to a higher intrinsic toxicity or a higher availability. Another study conducted on *Daphnia magna* observed a similar trend, but without statistical differences, leading the authors to conclude that these UV filters had similar toxic properties (Park et al., 2017).

The response measured in the AlamarBlue assay did not follow a sigmoid function as in the CFDA-AM and NR assay, but showed a hormetic dose-response relationship, which we previously observed following exposure to other toxicants (Carney Almoth et al., 2021; Lammel et al., 2013; Lammel and Navas, 2014). In the present study, fluorescence intensity values were found to increase in the range of 3.1–25 μ M to a maximum effect level of ~120–140% and then decrease again with further increasing concentrations dropping back to levels comparable to the unexposed control at 100 μ M (Fig. 3B). It is generally assumed that resazurine (i.e., the active ingredient of the AlamarBlue reagent) is intracellularly reduced to resorufin (i.e., the fluorescent product of resorufin) by reaction with reducing equivalents such as NADH and FADH₂ generated by the Krebs cycle, and thus, that a change in fluorescence intensity reflects a change in the cellular redox status/metabolic activity. According to this theory, our results suggest that exposure to low levels of organic UV filters stimulated cellular metabolic activity, which could reflect an adaptive response to counteract potential toxic effects. However, it must be kept in mind that resazurine might be reduced by mechanisms different to the one stated above. McMillian et al. (2001), for instance, suggested that resazurine reduction may occur through scavenging of electrons from lipid peroxidation cascades in dying cells (McMillian M et al., 2001), which could also be a plausible explanation in the present context.

Previous studies have demonstrated that EC50 values obtained with the RTgill-W1 cell assay generally correlate well with and can be used to predict fish acute toxicity (LC50, 96 h) (Fischer et al., 2019; Natsch et al., 2018; Tanneberger et al., 2013). The EC50s for avobenzone, octinoxate, and octocrylene determined in the present study are about 5–10 times lower than fish LC50s reported in databases (>100 mg/mL, 96 h limit test), probably because the stock solutions were prepared in DMSO, and this enhanced their solubility in the medium. This also explains why the LOECs determined for all tested organic UV filters were above their respective water solubility (Table 1). This is consistent with findings from regulatory testing, reporting no fish acute toxicity at concentrations below the limit of water solubility.

Comparing the effect levels caused by the inorganic UV filters with those caused by same mass concentrations of the organic UV filters (100 μ M of avobenzone, octinoxate, and octocrylene correspond to 31 μ g/mL, 29 μ g/mL, and 36 μ g/mL, respectively), our data seem to support the hypothesis that the former are less cytotoxic than the latter, though one needs to keep in mind that the NPs were not tested at concentrations > 10 μ g/mL to avoid interference issues, and the actual exposure dose of some of the substances, in particular the hydrophobic NPs, might deviate from their nominal dose (see discussion in 3.1.).

3.4. Interaction and combination effects of TiO₂ NP and organic UV filters

Fig. 4 shows the effects on RTgill-W1 cell viability caused by binary mixtures of specific TiO₂ NP and organic UV filters as determined by the CFDA-AM assay (kinetic analysis). Fig. 5 shows the results as determined with the NR assay. These two assays were least prone to NP interference because of the way relative cell viability is calculated and the additional washing steps and larger wavelengths used, respectively (cp. Section 2.7). Therefore, the results obtained by these assays were used as basis for the subsequent discussion. The results determined by means of the other two assays, that is, the classical CFDA-AM assay (endpoint

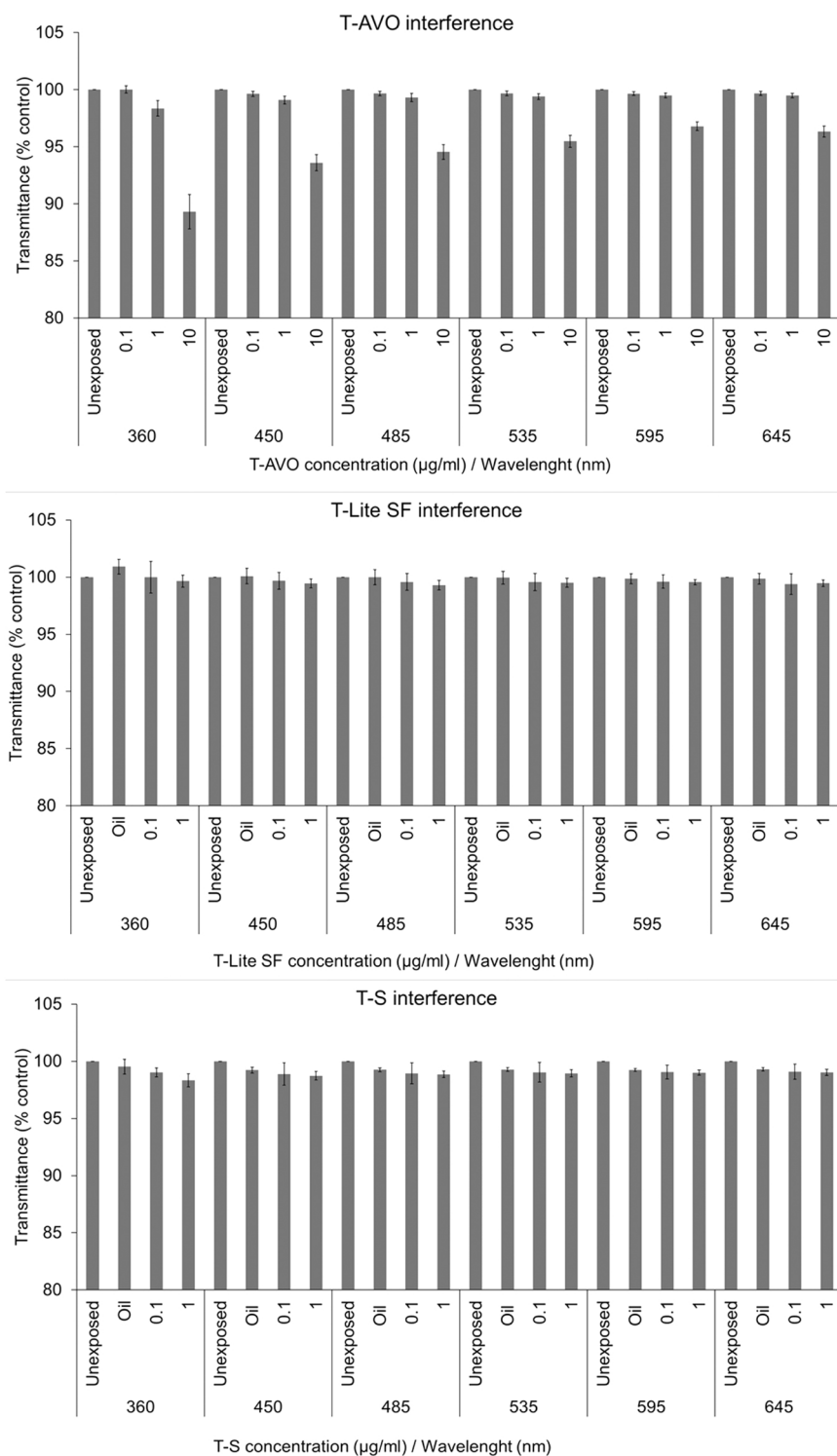


Fig. A9. NP-dependent attenuation of transmittance at excitation and emission wavelengths of fluorophores used in cell viability assays. Carboxyfluorescein (450 nm/485 nm), Resorufin (485 nm/535 nm), and NR (595 nm/645 nm). Measurements were conducted after washing with L-15/ex (2x). Note: Transmittance data are those shown in Table A but after normalisation to the unexposed control. Here they are presented again in form of a bar chart to illustrate the similarities to the trend observed in the cell viability assays (cp. Fig. 2). Cytotoxicity of octinoxate (range finding for WAF exposure experiment). Octinoxate exposure (concentration range: 0.39 – 100 µM, corresponding to 0.08 – 20.9 µg/mL) resulted in a dose-dependent decrease in RTgill-W1 cell viability as measured by the CFDA-AM assay (Fig. S1). The maximum decrease in cell viability was measured at 25 µM and was ~55%. Higher concentrations did not demonstrate higher cytotoxicity, probably because the compound’s solubility limit was reached/exceeded.

measurement) and AlamarBlue assay are shown in the appendix (Figs. A6 and A7).

3.4.1. CFDA-AM assay (kinetic analysis)

Fig. 4A shows that T-AVO reduced avobenzone toxicity. The effect was most pronounced in the treatments where cells were exposed to the highest avobenzone concentration. The effect observed for the mixture with the highest NP concentration (10 µg/mL) was found to be significantly different from that observed in the single substance treatment (i.e., the treatment with avobenzone alone). The same trend was observed

for the T-AVO-octinoxate mixture. Octinoxate toxicity was significantly reduced at the highest T-AVO concentration. Furthermore, the effect seemed to be NP concentration-dependent (Fig. 4B). Though antagonistic effects at the molecular/cellular level cannot be excluded, it is more likely that the decrease in organic UV filter toxicity was owed to a reduction of the test compounds’ availability due to binding to the NP. In the treatment where cells were exposed to the mixture of T-AVO and octocrylene, no interaction was observed, that is, the effect caused by the mixture was similar to the effect caused by the organic UV filter alone (Fig. 4C). With a logP of 7.1, octocrylene was the least hydrophilic

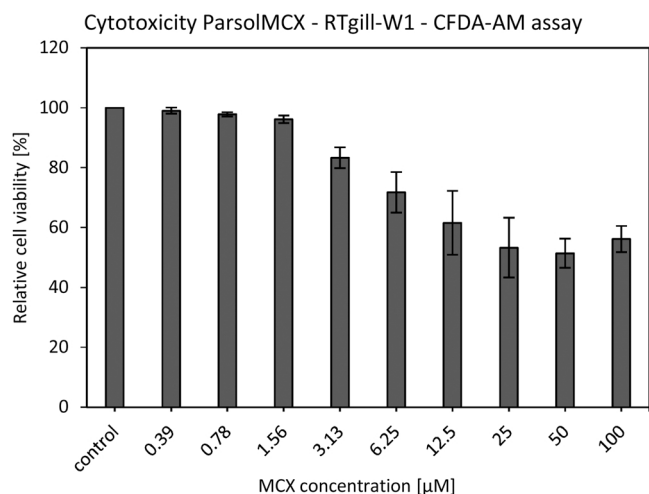


Fig. A10. Effect of octinoxate on RTgill-W1 cell viability as determined with the CFDA-AM assay (ranging finding experiment).

of the three tested organic UV filters, and therefore less likely to interact and bind to the hydrophilic SiO₂ coating of T-AVO, compared to avobenzone (logP = 4.8) and octinoxate (logP = 5.3). It is worth noting that the interaction of T-AVO with the organic UV filters could not be detected with the standard protocol of the CFDA-AM assay (Fig. A6), where relative cell viability is calculated based on fluorescence recorded in an endpoint measurement. In this assay, the NP-dependent effect on organic UV filter toxicity/availability was masked by the attenuation of fluorescence by NP interference (cp. Fig. 4 with Fig. A6).

For T-S and T-Lite SF, a similar trend like for T-AVO was observed, that is, a NP-dependent reduction in organic UV filter toxicity. However, it is difficult say if organic UV filter availability was reduced because of a direct interaction with the NPs or the oil/emulsifier solution, which although present in an only small percentage of (0.01%) in these treatments formed visible micelles/droplets.

3.4.2. NR assay

The results obtained in the NR assay, which was the assay least susceptible to NP interference, indicated no significant interaction between T-AVO and any of the organic UV filters, though it seemed that avobenzone toxicity/availability was slightly reduced in presence of the nanoparticulate UV filter. Furthermore, the reduction seemed to be NP-dose dependent, at least in the mixture containing the highest avobenzone concentrations, that is, 50 and 100 µM (Fig. 5A), which is largely consistent with our observations made with the modified CFDA-AM assay (see 3.4.1.).

Also for the organic UV filter mixtures containing T-Lite SF, the NR assay results showed a similar picture to the modified CFDA-AM assay, that is, a strong reduction of organic UV filter toxicity/availability, but no clear NP-dose dependent trend. This suggests that it was rather the dispersant, that is, the oil/emulsifier solution that affected organic UV filter toxicity/availability (Fig. 5D-F). The same general trend was observed for the mixture containing T-S (Fig. 5G-I). For the mixture with avobenzone, the NP dose-dependent effect was statistically significant (Fig. 5G). This suggests that, while the oil/emulsifier solution is responsible for a large part of the combination effect, the presence of the NPs may also contribute to modulating organic UV filter toxicity/availability.

The physico-chemical properties of the organic UV filters, such as their logP, appeared to have limited influence on the level of interaction with the NPs. For example, the differences in the levels of the combination effect caused by the mixture with the different types of TiO₂ NP UV filters (e.g., avobenzone+T-AVO, avobenzone+T-Lite SF, and avobenzone+T-S) were relatively small.

3.5. Exposure to water accommodated fraction of TiO₂ NP UV filters, organic UV filters, and mixtures

Testing the hydrophobic NPs, in particular together with the continuous oil phase used in sunscreen products, was methodologically challenging using the standard experimental design and dosing procedures (see 2.6.1. for experimental details). The main reasons for this were i) poor NP dispersibility/colloidal stability and ii) that the oil/emulsifier solution, which – although initially seeming to be well dispersed– formed micelles/droplets that separated again from the aqueous phase raising to surface the water column (medium), probably leading to concentration/entrapment of part of the nanomaterial, causing a decrease in availability and exposure dose. Therefore, we decided to conduct an additional set of experiments employing another experimental approach where we exposed the cells to only the WAF (see 2.6.2. for experimental details). This experimental approach had the disadvantage that the actual exposure concentrations for T-S and T-Lite SF likely deviated from the nominal concentrations, and were lower than that for T-AVO, for which no dispersibility/stability issue was observed. However, on the other hand, it increased realism with regard to exposure conditions prevailing in the environment. Of note, although we were not able to determine the TiO₂ concentration of the WAFs in this study, we expect that the percentage of TiO₂ in our samples (WAF) was in a similar range to that reported in Slomberg et al. (2021), where for a freshwater system, the maximum amount of T-S (introduced from the oil phase) recovered in the aqueous phase (i.e., WAF) was ~17.4%.

The results of this second set of experiments are shown in Fig. 6. Fig. 6B shows the results obtained in the CFDA-AM assay, and Fig. 6C shows the results obtained in the AlamarBlue assay. In the well plates that were exposed to aliquots sampled from the vials spiked with only the NPs (i.e., cell cultures treated with WAFs of T-AVO, T-Lite SF and T-S), a dose-dependent increase in fluorescence intensity was observed in the AlamarBlue assay, with the increase being highest for the WAF of T-S followed by the WAF of T-Lite SF and then the WAF of T-AVO (Fig. 6C). Resorufin-dependent fluorescence was increased in the oil-controls as well, but less than in the T-Lite SF and T-S treatments. As discussed previously (see Section 3.3), one explanation for this increase may be an increase in cellular metabolic activity as an adaptive response to low dose-exposure to toxic agents. Theoretically, an increase in fluorescence intensity could also reflect a higher cell number, that is, it could be indicative of a proliferation-stimulating effect, but given the short exposure duration (24 h) and the long cell-doubling time of RTgill-W1 cells (>24 h), this interpretation seems less plausible. Besides, NP-induced increase in cell number should also be reflected in the CFDA-AM assay, which was not the case (Fig. 6B). That acellular reduction of resazurine, i.e., a reduction via direct reaction with the applied nanomaterial caused or contributed to the higher fluorescence signal is also unlikely, as the respective interference test was negative, that is, incubation of T-AVO, T-Lite SF and T-S with AlamarBlue solution in absence of cells did not cause a noteworthy increase in fluorescence with respect to the AlamarBlue blank.

Unfortunately, it was not possible to determine whether any of the TiO₂ NP UV filters had a mitigating influence on octinoxate-induced toxicity as hypothesized, because the selected octinoxate concentration (6.25 µM) caused less toxicity in the WAF experiment (91.8 ± 3.4%) than in the previously conducted range finding experiments, where it caused about 50% of the maximum observed effect (Fig. A10). This discrepancy was unexpected and may be explained by a fraction of the originally dissolved amount of chemical being lost during the 48 h pre-incubation on the orbital shaker, possibly due to degradation, volatilization and or adsorption to the vial. In spite of this limitation, we made some interesting observations. As the AlamarBlue assay data in Fig. 6C show, octinoxate reversed the increase in fluorescence intensity caused by the TiO₂ NPs remaining in the WAFs. In addition, the extent of this “antagonistic” effect was noticeably higher for the WAFs of mixtures with either of the two hydrophobic NPs (T-Lite SF and T-S) than for

WAFs of the mixture containing the hydrophilic NP (T-AVO) (Fig. 6C). This observation let us speculate that the TiO₂ NP UV filters, especially the two hydrophobic types, might adsorb, i.e., enrich octinoxate at their surface rendering them more cytotoxic than their “clean” counterparts in the NP-only treatment. However, more research will need to be carried out to confirm this hypothesis.

As discussed earlier, it is possible that hydrophobic TiO₂ NP UV filters or NP-oil micelles raised to the surface resulting in a lower effective exposure dose, which could lead to effect underestimation. In order to account for this uneven vertical NP distribution in the culture vessel during the exposure, a hanging drop exposure was conducted in parallel, where the (same) WAFs were pipetted on top of cell monolayers cultured in 96-well plates, but the well plates were then incubated upside-down (cp. illustrations in Fig. 6A and D). The dose-response curves for the positive control were similar in the hanging drop-exposures and in the normal exposures (compare left and right graphs in Fig. 6), demonstrating that this methodological approach is viable. The hanging drop exposure to WAFs of T-AVO, T-Lite SF and T-S dispersions also yielded comparable results, showing that there were no significant differences in the vertical distribution/exposure concentrations of the test substances in the two exposure setups, and that the results obtained with the conventional exposure setup are reliable. We believe that in parallel-conducted hanging drop-exposures could be a possible strategy to obtain information on the toxicity of buoyant particles, which would otherwise (i.e., in the conventional exposure setup) not come in contact with the cells. Furthermore, the approach could be used to estimate the lowest and highest effect level, which may be caused by unstable NP dispersions for which characterisation of the exposure conditions is difficult/impossible and accurate toxicity estimates cannot be derived because of gravitational settling of NP agglomerates (In the conventional setup the cells would be exposed to both colloidal NPs and agglomerates subject to gravitational settling; In the hanging drop setup, the cells would be exposed to only the colloidal NP fraction).

4. Conclusions

This research has provided further evidence that NPs which absorb, scatter, and reflect light in the UV-Vis range, such as the tested TiO₂ NP UV filters, can interfere with fluorescence-based cell viability assays, and that such interference can lead to overestimation of NP toxicity, as well as hamper the detection and accurate determination of combination effects when testing NP-chemical mixtures. Herein, we have devised various strategies, which involved modifications of standard procedures for cell exposure, fluorescence measurement, and data analysis, which helped to estimate the level of interference and reduce the risk for misinterpreting effects observed for treatments containing NPs. Despite these improvements in the assay protocol, the interpretation of the data that were obtained for the two hydrophobic NPs tested, that is, the TiO₂ NP UV filters T-Lite SF and T-S, and their mixtures with organic UV filters remained challenging because of uncertainties about their size distribution and to-cell-delivered dose during exposure, resulting from their poor dispersibility and colloidal stability in aqueous media, as well as the formation of micelles by the oil-emulsifier solution (sunscreen oil), which was used to prepare NP stock dispersions and included in the testing to mimic the exposure scenario found in the environment. In spite of these limitations, we have been able to provide new insights into the toxicity of TiO₂ NP UV filters to fish gill cells (RTgill-W1 cell line), as well as their interaction and combination effects with organic UV filter substances, which are commonly used in sunscreens and with which they are likely to co-exist in the environment (avobenzone, octinoxate, and octocrylene). Our results suggest that T-AVO, T-Lite SF, and T-S are probably not acutely toxic to fish gill cells at environmentally relevant concentrations, and that they are less toxic than the tested organic UV filters. However, they appear to be surface chemistry-dependent differences in the interaction of T-AVO, T-Lite SF, and T-S with fish gill cells. Only T-AVO, that is, the TiO₂ NP UV filter comprising a

hydrophilic surface coating, has been found to be taken up by RTgill-W1 cells. In addition, our research has shown that mixtures of TiO₂ NP UV filters and organic UV filters may have a different toxicological profile compared to the single substances (i.e., the mixture components), but probably do not pose an increased hazard, as the presence of NPs (and in the case of T-S and T-Lite SF, as well the presence of oil micelles) rather tends to decrease organic UV filter toxicity, probably by reducing their availability through sorption of the compound to their surface. Furthermore, our findings seem to support the hypothesis that the magnitude of this effect may depend on the degree of hydrophobic/hydrophilic interactions between the NP surface and the chemical compound.

CRedit authorship contribution statement

Nicolas Martin: Investigation, Methodology, Formal analysis, Validation, Data curation, Writing - original draft, Writing - review & editing, Visualization. **Britt Wassmur:** Investigation, Formal analysis, Data curation. **Danielle Slomberg:** Resources, Writing - review & editing. **Jérôme Labille:** Resources, Writing -review & editing. **Tobias Lammel:** Funding acquisition, Project administration, Supervision, Conceptualization, Methodology, Investigation, Formal analysis, Validation, Data curation, Visualization. Writing original draft, Writing - review & editing.

Declaration of Competing Interest

The authors declare the following financial interests/personal relationships which may be considered as potential competing interests: Tobias Lammel reports financial support was provided by Swedish Research Council Formas. Tobias Lammel reports financial support was provided by German Research Foundation. Tobias Lammel reports financial support was provided by Stiftelsen Wilhelm och Martina Lundgrens Vetenskapsfond. Tobias Lammel reports financial support was provided by Helge Axelsson Johnsons Stiftelse.

Acknowledgements

The present study received financial support from the Swedish Research Council for Environment, Agricultural Sciences and Spatial Planning FORMAS (Grant 2016–00742), the German Research Foundation (DFG Research Fellowship/Project 276093679), Helge Axelsson Johnsons Stiftelse (Grant F20–0491), and Stiftelsen Wilhelm och Martina Lundgrens Vetenskapsfond (Grant 253157706). Nicolas Martin was financially supported by the AMI grant program from the University of Montpellier. The authors acknowledge the Centre for Cellular Imaging (CCI) at the University of Gothenburg and the National Microscopy Infrastructure, NMI (VR-RFI 2016–00968) for providing assistance with electron microscopy.

Appendix

See Appendix [Table A1](#), [Table A2](#).

See Appendix [Fig. A1](#), [Fig. A2](#), [Fig. A3](#), [Fig. A4](#), [Fig. A5](#), [Fig. A6](#), [Fig. A7](#), [Fig. A8](#), [Fig. A9](#), [Fig. A10](#).

References

- Araújo, M.J., et al., 2018. Effects of UV filter 4-methylbenzylidene camphor during early development of *Solea senegalensis* Kaup, 1858. *Sci. Total Environ.* 628–629, 1395–1404.
- Barone, A.N., et al., 2019. Acute toxicity testing of TiO₂-based vs. oxybenzone-based sunscreens on clownfish (*Amphiprion ocellaris*). *Environ. Sci. Pollut. Res. Int.* 26, 14513–14520.
- Bols, N.C., et al., 1994. Development of a cell line from primary cultures of rainbow trout, *Oncorhynchus mykiss* (Walbaum), gills. *J. Fish. Dis.* 17, 601–611.
- Bols, N.C., et al., 2005. Chapter 2 Use of fish cell lines in the toxicology and ecotoxicology of fish. *Piscine cell lines in environmental toxicology*. In:

- Mommsen, T.P., Moon, T.W. (Eds.), *Biochemistry and Molecular Biology of Fishes*. Elsevier, pp. 43–84.
- Book, F., et al., 2019. Ecotoxicity screening of seven different types of commercial silica nanoparticles using cellular and organismic assays: Importance of surface and size. *NanoImpact* 13, 100–111.
- Carney Almroth, B., et al., 2021. Assessing the effects of textile leachates in fish using multiple testing methods: From gene expression to behavior. *Ecotoxicol. Environ. Saf.* 207, 111523.
- Carvalho, A., et al., 2021. Mild effects of sunscreen agents on a marine flatfish: oxidative stress, energetic profiles, neurotoxicity and behaviour in response to titanium dioxide nanoparticles and oxybenzone. *Int. J. Mol. Sci.* 22, 1567.
- Catalano, R., et al., 2020a. Safety evaluation of TiO₂ nanoparticle-based sunscreen UV filters on the development and the immunological state of the sea urchin *paracentrotus lividus*. *Nanomaterials* 10, 2102.
- Catalano, R., et al., 2020b. Optimizing the dispersion of nanoparticulate TiO₂-based UV filters in a non-polar medium used in sunscreen formulations – The roles of surfactants and particle coatings. *Colloids Surf. A: Physicochem. Eng. Asp.* 599, 124792.
- Chatelain, E., Gabard, B., 2001. Photostabilization of butyl methoxydibenzoylmethane (Avobenzone) and ethylhexyl methoxycinnamate by bis-ethylhexyloxyphenol methoxyphenyl triazine (Tinosorb S), a new UV broadband filter. *Photochem. Photobiol.* 74, 401–406.
- Dayeh, V.R., et al., 2003. The use of fish-derived cell lines for investigation of environmental contaminants. *Curr. Protoc. Toxicol.* Chapter 1. Unit 1.5.
- DiNardo, J.C., Downs, C.A., 2018. Dermatological and environmental toxicological impact of the sunscreen ingredient oxybenzone/benzophenone-3. *J. Cosmet. Dermatol.* 17, 15–19.
- Diniz, M.S., et al., 2013. Liver alterations in two freshwater fish species (*Carassius auratus* and *Danio rerio*) following exposure to different TiO₂ nanoparticle concentrations. *Microsc. Microanal.* 19, 1131–1140.
- Egambaram, O.P., et al., 2020. Materials science challenges in skin UV protection: a review. *Photochem. Photobiol.* 96, 779–797.
- Emnet, P., et al., 2015. Personal care products and steroid hormones in the Antarctic coastal environment associated with two Antarctic research stations, McMurdo Station and Scott Base. *Environ. Res.* 136, 331–342.
- Faure, B., et al., 2013. Dispersion and surface functionalization of oxide nanoparticles for transparent photocatalytic and UV-protecting coatings and sunscreens. *Sci. Technol. Adv. Mater.* 14, 023001.
- Federici, G., et al., 2007. Toxicity of titanium dioxide nanoparticles to rainbow trout (*Oncorhynchus mykiss*): Gill injury, oxidative stress, and other physiological effects. *Aquat. Toxicol.* 84, 415–430.
- Fischer, M., et al., 2019. Repeatability and reproducibility of the RTgill-W1 cell line assay for predicting fish acute toxicity. *Toxicological Sci.* 169, 353–364.
- Fouqueray, M., et al., 2013. Exposure of juvenile *Danio rerio* to aged TiO₂ nanomaterial from sunscreen. *Environ. Sci. Pollut. Res.* 20, 3340–3350.
- Gago-Ferrero, P., et al., 2012. An overview of UV-absorbing compounds (organic UV filters) in aquatic biota. *Anal. Bioanal. Chem.* 404, 2597–2610.
- Gaspar, L.R., Maia Campos, P.M.B.G., 2006. Evaluation of the photostability of different UV filter combinations in a sunscreen. *Int. J. Pharm.* 307, 123–128.
- Gerloff, K., et al., 2017. The adverse outcome pathway approach in nanotoxicology. *Comput. Toxicol.* 1, 3–11.
- Goksoyr, A., et al., 2009. Balsa raft crossing the Pacific finds low contaminant levels. *Environ. Sci. Technol.* 43, 4783–4790.
- Gondikas, A., et al., 2018. Where is the nano? Analytical approaches for the detection and quantification of TiO₂ engineered nanoparticles in surface waters. *Environ. Sci.: Nano* 5, 313–326.
- Gondikas, A.P., et al., 2014. Release of TiO₂ Nanoparticles from Sunscreens into Surface Waters: A One-Year Survey at the Old Danube Recreational Lake. *Environ. Sci. Technol.* 48, 5415–5422.
- Hao, L., et al., 2009. Effect of sub-acute exposure to TiO₂ nanoparticles on oxidative stress and histopathological changes in Juvenile Carp (*Cyprinus carpio*). *J. Environ. Sci.* 21, 1459–1466.
- Horie, M., Sugino, S., Kato, H., Tabei, Y., Nakamura, A., Yoshida, Y., 2016. Does photocatalytic activity of TiO₂ nanoparticles correspond to photo-cytotoxicity? Cellular uptake of TiO₂ nanoparticles is important in their photo-cytotoxicity. *Toxicol. Mech. Methods* 26 (4), 284–294.
- Iliina, S.M., et al., 2017. Investigations into titanium dioxide nanoparticle and pesticide interactions in aqueous environments. *Environ. Sci.: Nano* 4, 2055–2065.
- Johnson, A.C., et al., 2011. An assessment of the fate, behaviour and environmental risk associated with sunscreen TiO₂ nanoparticles in UK field scenarios. *Sci. Total Environ.* 409, 2503–2510.
- Johnston, B.D., et al., 2010. Bioavailability of nanoscale metal oxides TiO₂, CeO₂, and ZnO to Fish. *Environ. Sci. Technol.* 44, 1144–1151.
- Jovanovic, B., 2015. Review of titanium dioxide nanoparticle phototoxicity: developing a phototoxicity ratio to correct the endpoint values of toxicity tests. *Toxicol. Chem.* 34, 5.
- Jurado, A., et al., 2014. Urban groundwater contamination by residues of UV filters. *J. Hazard. Mater.* 271, 141–149.
- Kim, S., Choi, K., 2014. Occurrences, toxicities, and ecological risks of benzophenone-3, a common component of organic sunscreen products: A mini-review. *Environ. Int.* 70, 143–157.
- Kunz, P.Y., Fent, K., 2006. Estrogenic activity of UV filter mixtures. *Toxicol. Appl. Pharmacol.* 217, 86–99.
- Labille, J., et al., 2020. Assessing UV filter inputs into beach waters during recreational activity: A field study of three French Mediterranean beaches from consumer survey to water analysis. *Sci. Total Environ.* 706, 136010.
- Lammel, T., et al., 2013. Internalization and cytotoxicity of graphene oxide and carboxyl graphene nanoplatelets in the human hepatocellular carcinoma cell line Hep G2. *Part Fibre Toxicol.* 10 (27).
- Lammel, T., et al., 2019a. Endocytosis, intracellular fate, accumulation, and agglomeration of titanium dioxide (TiO₂) nanoparticles in the rainbow trout liver cell line RTL-W1. *Environ. Sci. Pollut. Res.* 26, 15354–15372.
- Lammel, T., et al., 2019b. Mixture toxicity effects and uptake of titanium dioxide (TiO₂) nanoparticles and 3,3',4,4'-tetrachlorobiphenyl (PCB77) in juvenile brown trout following co-exposure via the diet. *Aquat. Toxicol. (Amst., Neth.)* 213, 105195.
- Lammel, T., Navas, J.M., 2014. Graphene nanoplatelets spontaneously translocate into the cytosol and physically interact with cellular organelles in the fish cell line PLHC-1. *Aquat. Toxicol.* 150, 55–65.
- Lammel, T., Sturve, J., 2018. Assessment of titanium dioxide nanoparticle toxicity in the rainbow trout (*Oncorhynchus mykiss*) liver and gill cell lines RTL-W1 and RTgill-W1 under particular consideration of nanoparticle stability and interference with fluorometric assays. *NANOIMPACT* 11, 1–19.
- Li, M., et al., 2020. Effects of mixtures of engineered nanoparticles and metallic pollutants on aquatic organisms. *Environments* 7, 27.
- Liu, H., et al., 2019. Toxicity responses of different organs of zebrafish (*Danio rerio*) to silver nanoparticles with different particle sizes and surface coatings. *Environ. Pollut.* 246, 414–422.
- Liu, J.-L., Wong, M.-H., 2013. Pharmaceuticals and personal care products (PPCPs): a review on environmental contamination in China. *Environ. Int.* 59, 208–224.
- Mandal, S.C., et al., 2020. Polarized trout epithelial cells regulate transepithelial electrical resistance, gene expression, and the phosphoproteome in response to viral infection. *Front. Immunol.* 11.
- McMillan, M., et al., 2001. Publication No.: WO/2001/098531. Publication Date. Resazurin-based cytotoxicity assay, 27. World Intellectual Property Organization (WIPO), Geneva, Switzerland, p. 2001. Publication No.: WO/2001/098531. Publication Date.
- Miao, W., et al., 2015. Effects of titanium dioxide nanoparticles on lead bioconcentration and toxicity on thyroid endocrine system and neuronal development in zebrafish larvae. *Aquat. Toxicol.*
- Natsch, A., et al., 2018. Accurate prediction of acute fish toxicity of fragrance chemicals with the RTgill-W1 cell assay. *Environ. Toxicol. Chem.* 37, 931–941.
- Osterwalder, U., et al., 2014. Global state of sunscreens. *Photodermatol., Photoimmunol. Photomed.* 30, 62–80.
- Park, C.B., et al., 2017. Single- and mixture toxicity of three organic UV-filters, ethylhexyl methoxycinnamate, octocrylene, and avobenzone on *Daphnia magna*. *Ecotoxicol. Environ. Saf.* 137, 57–63.
- Qiang, L., et al., 2016. Effects of nano-TiO₂ on perfluorooctanesulfonate bioaccumulation in fishes living in different water layers: Implications for enhanced risk of perfluorooctanesulfonate. *Nanotoxicology* 10, 471–479.
- Ramos, S., et al., 2015. Advances in analytical methods and occurrence of organic UV-filters in the environment — A review. *Sci. Total Environ.* 526, 278–311.
- Ramos, S., et al., 2016. A review of organic UV-filters in wastewater treatment plants. *Environ. Int.* 86, 24–44.
- Reed, R.B., et al., 2017. Multi-day diurnal measurements of Ti-containing nanoparticle and organic sunscreen chemical release during recreational use of a natural surface water. *Environ. Sci.: Nano* 4, 69–77.
- Reeves, J.F., et al., 2008. Hydroxyl radicals (OH) are associated with titanium dioxide (TiO₂) nanoparticle-induced cytotoxicity and oxidative DNA damage in fish cells. *Mutat. Res. /Fundam. Mol. Mech. Mutagen.* 640, 113–122.
- Sánchez Rodríguez, A., et al., 2015. Occurrence of eight UV filters in beaches of Gran Canaria (Canary Islands). An approach to environmental risk assessment. *Chemosphere* 131, 85–90.
- Sánchez-Quiles, D., Tovar-Sánchez, A., 2015. Are sunscreens a new environmental risk associated with coastal tourism? *Environ. Int.* 83, 158–170.
- Sanders, K., Degen, L.L., Mundy, W.R., Zucker, R.M., Dreher, K., Zhao, B., Boyes, W.K., 2012. In vitro phototoxicity and hazard identification of nano-scale titanium dioxide. *Toxicol. Appl. Pharmacol.* 258 (2), 226–236.
- Schirmer, K., et al., 1997. Methodology for demonstrating and measuring the photocytotoxicity of fluoranthene to fish cells in culture. *Toxicol. Vitro* 11, 107–119.
- Schlumpf, M., et al., 2001. In vitro and in vivo estrogenicity of UV screens. *Environ. Health Perspect.* 109, 239–244.
- Schnell, S., et al., 2016. Procedures for the reconstruction, primary culture and experimental use of rainbow trout gill epithelia. *Nat. Protoc.* 11, 490–498.
- Shi, X., et al., 2016. Fate of TiO₂ nanoparticles entering sewage treatment plants and bioaccumulation in fish in the receiving streams. *NanoImpact* 3–4, 96–103.
- Slomberg, D.L., et al., 2021. Release and fate of nanoparticulate TiO₂ UV filters from sunscreen: Effects of particle coating and formulation type. *Environ. Pollut.* 271, 116263.
- Stern, S.T., et al., 2012. Autophagy and lysosomal dysfunction as emerging mechanisms of nanomaterial toxicity. *Part. Fibre Toxicol.* 9, 20.
- Sun, H., et al., 2007. Enhanced accumulation of arsenate in carp in the presence of titanium dioxide nanoparticles. *Water, Air, Soil Pollut.* 178, 245–254.
- Tang, Y., Cai, R., Cao, D., Kong, X., Lu, Y.B., 2018. Photocatalytic production of hydroxyl radicals by commercial TiO₂ nanoparticles and phototoxic hazard identification. *Toxicology* 406, 1–8.
- Tanneberger, K., et al., 2013. Predicting Fish Acute Toxicity Using a Fish Gill Cell Line-Based Toxicity Assay. *Environmental Science & Technology* 47, 1110–1119.
- Tovar-Sánchez, A., et al., 2013. Sunscreen products as emerging pollutants to coastal waters. *PLOS ONE* 8, e65451.
- Trubitt, R.T., et al., 2015. Transepithelial resistance and claudin expression in trout RTgill-W1 cell line: Effects of osmoregulatory hormones. *Comp. Biochem. Physiol. Part A: Mol. Integr. Physiol.* 182, 45–52.

- Tsui, M.M.P., et al., 2014. Occurrence, distribution and ecological risk assessment of multiple classes of UV filters in surface waters from different countries. *Water Res.* 67, 55–65.
- Turan, N.B., et al., 2019. Nanoparticles in the aquatic environment: usage, properties, transformation and toxicity - A review. *Process Saf. Environ. Prot.* 130, 238–249.
- Urbach, F., 2001. The historical aspects of sunscreens. *J. Photochem. Photobiol. B: Biol.* 64, 99–104.
- Villalobos-Hernández, J.R., Müller-Goymann, C.C., 2006. Sun protection enhancement of titanium dioxide crystals by the use of carnauba wax nanoparticles: the synergistic interaction between organic and inorganic sunscreens at nanoscale. *Int. J. Pharm.* 322, 161–170.
- Wang, Z., et al., 2016. Trophic transfer and accumulation of TiO₂ nanoparticles from clamworm (*Perinereis aibuhitensis*) to juvenile turbot (*Scophthalmus maximus*) along a marine benthic food chain. *Water Res.* 95, 250–259.
- Wissing, S.A., Müller, R.H., 2001. Solid lipid nanoparticles (SLN)—a novel carrier for UV blockers. *Die Pharm.* 56, 783–786.
- Xiong, D., et al., 2011. Effects of nano-scale TiO₂, ZnO and their bulk counterparts on zebrafish: Acute toxicity, oxidative stress and oxidative damage. *Sci. Total Environ.* 409, 1444–1452.
- Xiong, S.J., George, S.J., Ji, Z.X., Lin, S.J., Yu, H.Y., Damoiseaux, R., Loo, S.C.J., 2013. Size of TiO₂ nanoparticles influences their phototoxicity: an in vitro investigation. *Arch. Toxicol.* 87 (1), 99–109.
- Yin, J.J., Liu, J., Ehrenshaft, M., Roberts, J.E., Fu, P.P., Mason, R.P., Zhao, B.Z., 2012. Phototoxicity of nano titanium dioxides in HaCaT keratinocytes-Generation of reactive oxygen species and cell damage. *Toxicol. Appl. Pharmacol.* 263, 1.
- Ylä-Mononen, L., Decision on substance evaluation. ECHA, 2018.**
- Zhang, X., et al., 2007. Enhanced bioaccumulation of cadmium in carp in the presence of titanium dioxide nanoparticles. *Chemosphere* 67, 160–166.
- Zhao, J., Stenzel, M.H., 2018. Entry of nanoparticles into cells: the importance of nanoparticle properties. *Polym. Chem.* 9, 259–272.